GEOLOGICAL SURVEY OF CANADA
OPEN FILE 6313

The Flin Flon 3D Knowledge Cube

E. Schetselaar, S. Pehrsson, C. Devine, M. Currie, D. White and M. Malinowski

2010

Natural Resources Canada | Ressources naturelles Canada

Canada

GEOLOGICAL SURVEY OF CANADA
OPEN FILE 6313

The Flin Flon 3D Knowledge Cube

E. Schetselaar, S. Pehrsson, C. Devine, M. Currie, D. White and M. Malinowski

2010

This publication is available from the Geological Survey of Canada Bookstore (http://gsc.nrcan.gc.ca/bookstore_e.php).
It can also be downloaded free of charge from GeoPub
(http://geopub.nrcan.gc.ca/).

Schetselaar, E., Pehrsson, S., Devine, C., Currie, M., White, D. and Malinowski, M., 2010. The Flin Flon 3D Knowledge Cube, Geological Survey of Canada, Open File 6313, 35 p.

TABLE OF CONTENTS

SUMMARY

A 3D geologic model of the Flin Flon exploration camp has been compiled from integrated analyses of drill core, 2D and 3D seismic, mine survey and geological map data. The 3D model is built from a series of lithostratigraphic and fault surfaces which are, together with their underpinning drill hole and map constraints, represented in a '3D knowledge cube'. The geometry and attitude of the 3D lithostratigraphic surfaces, and their topological relationships with multiple generations of shear zones and thrust faults, suggest that the Flin Flon exploration camp is underlain by an E-dipping stack of W-vergent thrust imbricates formed by post- and possibly pre-Missi deformation events. The imbricate stack was subsequently deformed by E-trending ductile thrust faults that internally imbricated the Flin Flon arc assemblage and Missi sedimentary rocks and brought up rocks of the former against the latter in a northerly direction. The VMS-hosting Millrock member has been stacked on at least four structural levels, enhancing the VMS potential in the footwall and hanging wall vicinities of the known ore deposits where both thrust systems intersect. N-trending post-metamorphic subvertical faults have further segmented the polyphase imbricate stack, complicating the correlation of lithostratigraphic successions across them.

INTRODUCTION

A central objective of the Geological Survey of Canada's third Targeted Geoscience Initiative Program (TGI3) was to update the geoscience knowledge base in several VMS exploration camps across Canada. Toward this objective, a 3D geological modelling initiative was undertaken to enhance insight in the geological setting of the 85.5 million tonne (Mt) Flin Flon-Callinan-777 VMS ore system hosted in the Paleoproterozoic Flin Flon Belt of Central Manitoba and Saskatchewan. The 3D modelling results have been compiled in a 3D 'knowledge cube' *i.e.* a 3D geological model that consists of key lithostratigraphic and fault surfaces constrained by integrated analysis of drill hole, seismic, mine survey and geological map data. The 3D modelling work reported in this Open File document was supported by other TGI3 initiatives undertaken at Flin Flon, which involved the acquisition and interpretation of 2D and 3D seismic data (Malinowski et al., *in prep.*) and the cross-provincial boundary TGI3 Flin Flon geological mapping project (Simard et al., 2010).

GEOLOGY

Regional geological setting

The Flin Flon Belt is part of the Paleoproterozoic Flin Flon-Glennie complex, a collage of accreted oceanic terranes between the Archean Hearne, Sask and Superior cratons (Fig. 1, inset) that obducted during the collisional stages of the Trans-Hudson orogeny between ca. 1.84 Ga and 1.80 Ga (Corrigan et al., 2009 and references therein). It comprises 1.92-1.88 Ga volcanic island arc, back-arc basin and ocean floor assemblages stitched by 1.87-1.84 Ga successor arc plutons and overlain by 1.84-1.83 Ga flysch and molasse basin sequences. The Flin Flon-Glennie complex consists of four main structural entities, which from west to east are the Glennie Domain, Hanson Lake block, Amisk collage and Snow Lake arc assemblage (Fig. 1).

The Flin Flon exploration camp is located in the Amisk collage (Fig. 1), a 70 km wide belt of basalt-dominated volcanic, volcaniclastic, synvolcanic intrusive and subordinate felsic volcanic rocks assigned to regional fault-bounded juvenile arc, ocean floor and ocean plateau tectonostratigraphic assemblages on the basis of whole rock and trace element geochemical analyses (Stern et al., 1995; Syme et al., 1999). The Amisk collage is structurally subdivided in fault-bounded

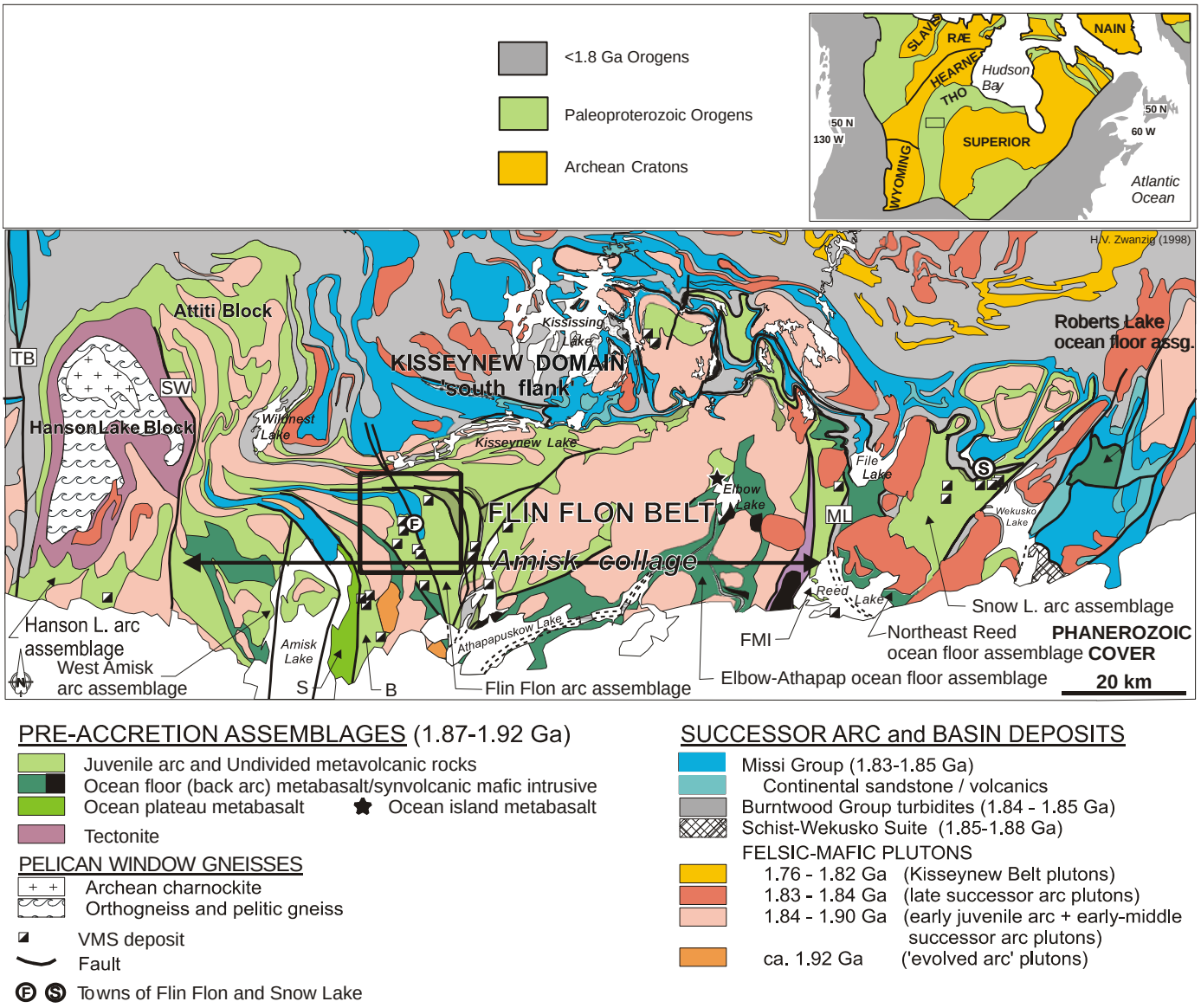

Figure 1. Tectonic assemblage map of the Flin Flon Belt (after Galley et al., 2007 and references therein), illustrating the tectonostratigraphic assemblages, the location of the various accretionary assemblages, and major mineral deposits. B=Birch Lake assemblage; FMI=Fourmile Island assemblage; ML=Morton Lake fault zone; S=Sandy Bay assemblage; TB=Tabernor fault zone. The box shows the location of the Flin Flon exploration camp.

blocks, across which lithostratigraphic correlation is uncertain or impossible to establish (Lucas et al., 1999). The Amisk collage is intruded by ca. 1.87 – 1.83 Ga successor arc mafic and felsic plutons and unconformably overlain by the Missi Group, a sequence of clastic metasedimentary rocks of fluvial and alluvial origin (Syme and Bailes, 1993). The Flin Flon Belt is richly endowed with VMS deposits that are exclusively hosted in juvenile arc assemblages (Syme et al., 1999). The central Flin Flon Belt is characterized by sub-greenschist to greenschist metamorphic facies reaching the biotite isograd (Bailes and Syme, 1989).

Geology of the Flin Flon exploration camp

The Flin Flon mine camp is centered on the 85.5 Mt Flin Flon-Callinan-777 VMS ore system and straddles the border between the provinces of Saskatchewan and

Manitoba. The mines in the camp are currently owned and operated by Hudson Bay Mining and Smelting Company Limited (a subsidiary of HudBay Minerals Inc.). Figure 2 shows a generalized geologic map and schematic lithostratigraphic section of the area covered by the TGI3 Flin Flon mapping project (Simard et al., 2010). This area is located in the western Flin Flon arc assemblage (Fig. 1) and underlain by the eastern Flin Flon- and western margin of the Hook Lake blocks (Fig. 2) (Lucas et al., 1999).

The 1:10 000 scale TGI3 (Simard et al., 2010) and previous geological mapping projects (Ames et al., 2002; Ames et al., 2003; Gibson et al., 2003; Devine et al., 2002; Devine, 2003; DeWolfe, 2008) have resulted in a refined description of the lithostratigraphy of the Flin Flon arc assemblage. Three informal formations and further subdivisions into members have been defined in the Flin Flon block (Fig. 2b) that can be correlated across the Saskatchewan-Manitoba provincial boundary (MacLachlan and Devine, 2007; Simard et al., 2010). These include from oldest to youngest the Flin Flon, Hidden and Louis formations (Fig. 2b). The 62.5 Mt Flin Flon Main, 8.4 Mt Callinan and 14.5 Mt 777 VMS deposits (Galley et al., 2007) are hosted in rhyolite flows, rhyolite breccia and bedded tuff of the Millrock member that separates the footwall basalt and mafic volcaniclastic succession of the Flin Flon formation from the hanging wall basalt-dominated successions of the Hidden and Louis formations (Fig. 2b). The footwall of the ore system (base of the Millrock member) shows an abrupt lateral transition in lithofacies at the Flin Flon mine shaft from intact pillowed basalt flows in the south to a thick volcaniclastic-dominated succession consisting of megabreccia, pillow fragment breccia and lapilli tuff towards the north (Fig. 2a). This abrupt lateral change in lithofacies marks the transition from the margin to the proximal infill of an intra-arc rift basin or cauldron (Syme and Bailes, 1993; Devine et al., 2002; Gibson et al., 2009).

The volcanic and volcaniclastic lithostratigrapy of the western Hook Lake block is also interpreted to contain products of proximal reworking deposited in a subsidence structure and/or basin (Kremer and Simard, 2007). It comprises steeply E-dipping and W-facing overturned fault-bounded panels of mafic volcanic and volcaniclastic rocks south and west of the E-dipping Cliff Lake tonalite stock that partly dips underneath it (Fig. 2). The reworked volcanic rocks consist of heterolithic mafic to mafic-felsic tuff breccia interlayered with pillowed plagioclase $\pm$ pyroxene phyric basaltic flows and overlain by aphyric to strongly feldspar-phyric basalt flows with associated volcaniclastic rocks. This succession is juxtaposed by faults against successions of aphyric to plagioclase $\pm$ pyroxene phyric basaltic flows with intercalations of massive quartz-phyric rhyolite at their base (Kremer and Simard, 2007).

A narrow fault block of volcanic, volcaniclastic and intrusive rocks, east of the Mandy Road fault and west of the Cliff Lake fault, separates the Flin Flon block from the Hook Lake block, directly south of the fold interference basin that contains fluvial deposits of the Missi Group (Missi structural basin, Fig. 2a). This block, which hosts the earliest mined VMS deposits (Schist and Mandy deposits, Fig. 2a) of the Flin Flon Belt (Galley et al., 2007), has to date not been assigned to any of the known lithographic successions of the Flin Flon arc assemblage (Simard et al., 2010). The rocks exposed in this fault-bounded steeply dipping panel dominantly consist of heterolithic to mafic tuff breccias and fine-grained mafic volcaniclastic rocks with subordinate felsic volcaniclastic, mafic and felsic extrusive rocks (Simard, 2006; Cole et al., 2008). Drill holes along its northern strike extent intersect an E-dipping imbricate of hydrothermally altered, sparsely mineralized basalt and minor volcaniclastic and felsic volcanic rocks thrust amidst sandstone of the Missi Group that is exposed east of Ross Lake, where the sulphide mineralization within it is known as the 'Lake View showing' (Hudbay Minerals Inc, *pers. comm.*; LVS, Fig. 2a). This imbricate could also not be assigned with any level of certainty to the known lithostratigraphic units of the Flin Flon arc assemblage (Simard et al., 2010, Fig. 2b).

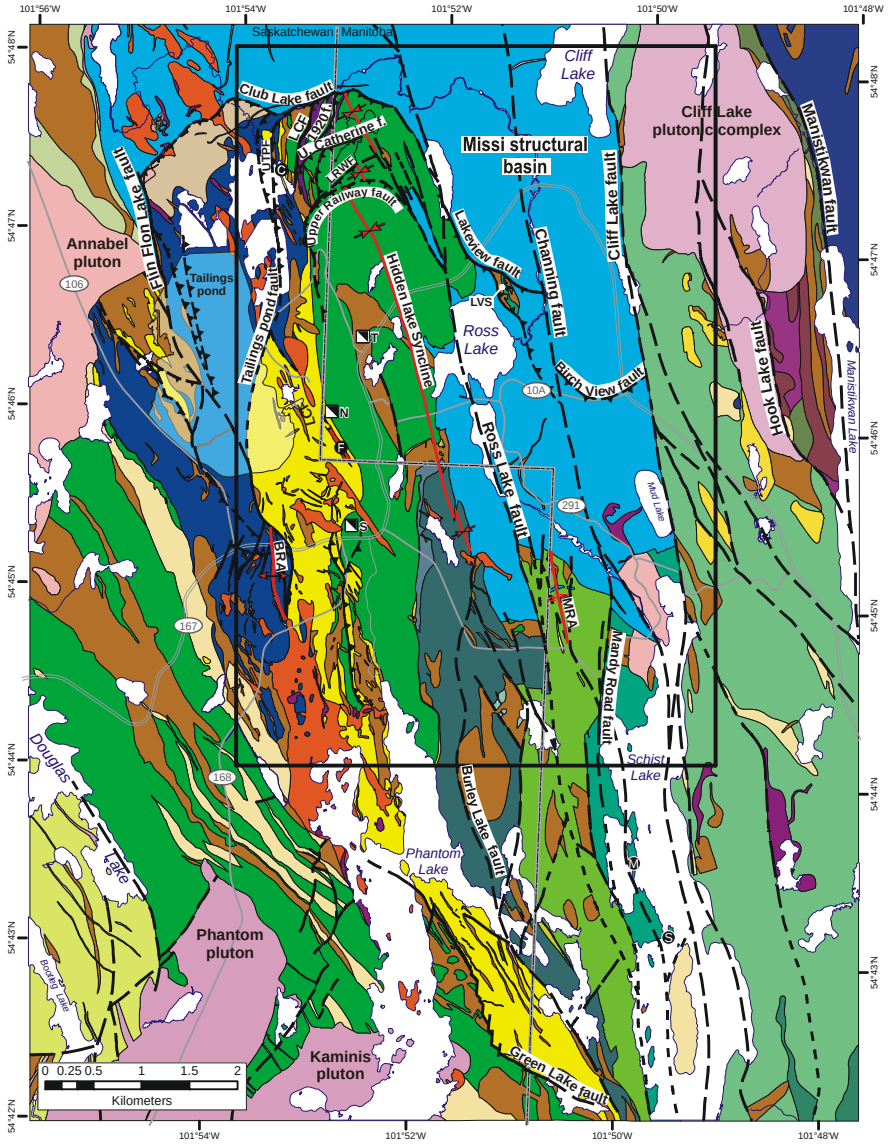

faults
- approximate
- defined

C VMS deposit
C - Callinan
T - Triple 7
F - Flin Flon
M - Mandy
S - Schist Lake

Mine Shaft
T - Triple 7
N - North Main
S - South Main

Missi Group

SUCCESSOR ARC ROCKS
- 'Late' intrusions
- Boundary intrusions
- Phantom Lake intrusion

Pre-Missi intrusions (Annabel, Channing)

FLIN FLON ARC ASSEMBLAGE (>1.88 Ga)

Flin Flon Block

Douglas formation
- Undivided mafic volcanic and felsic volcaniclastic rocks

Hamell Lake volcanic rocks

Louis formation
- undivided mafic volcanic rocks
- Icehouse member
- Tower member

Unassigned mafic volcanic and heterolithic volcaniclastic rocks

Hidden formation
- 1920 unit
- Carlisle Lake member
- Reservoir Member
- Stockwell member

Flin Flon formation
- Massive sulfide: Cu-Zn
- Millrock member
- Blue Lagoon member
- Club member

Hook Lake Block
- Western felsic volcanic rocks
- Western mafic volcanic rocks
- Western volcaniclastic rocks
- Eastern mafic volcanic rocks
- Eastern Felsic volcanic rocks
- Eastern Volcaniclastics

Cope Lake Block
- Undivided mafic volcanic and volcaniclastic rocks

Synvolcanic intrusions
- Cliff Lake pluton
- Mikanagan Lake Sill related intrusions
- Mafic dykes and sills
- Felsic dykes and sills

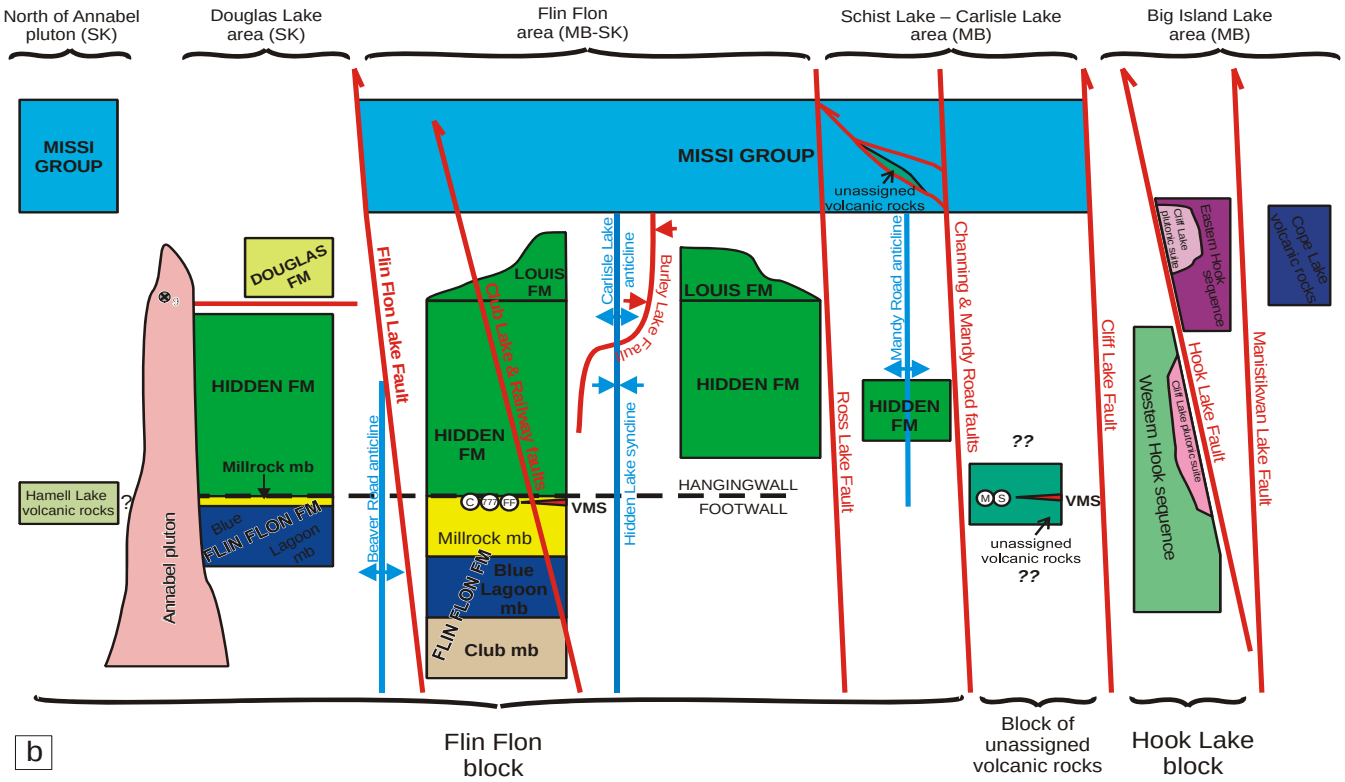

Note: All fold structures shown on this schematic stratigraphic figure, including the Burley Lake Fault (a faulted syncline), are pre-Missi in age. For simplicity, post-Missi fold structures and strike-slip reactivation of the thrust faults are not shown. Red lines represent faults, blue lines represent folds, coloured arrows represent facing directions on each side of a given structure. (VMS: volcanogenic massive sulphide deposits, C: Callinan, FF: Flin Flon, M: Mandy, S: Schist Lake)

Figure 2. (a) (opposite page) Geological map of the Flin Flon exploration camp generalized from the 1:10 000 scale TGI3 geological map (modified after Simard et al., 2010); LRF = Lower Railway fault, LCF = Lower Catherine fault, UTPF = Upper Tailings Pond fault, BRA = Beaver Road anticline, MRA = Mandy Road anticline, LVS = Lake View Showing. The rectangle outlines the surface projection of the knowledge cube; (b) Schematic E-W section showing lithostratigraphy, regional fold and fault structures of the eastern Flin Flon and western Hook Lake blocks (modified after Simard et al., 2010).

The Flin Flon arc assemblage is intruded by the ca. 1.87 - 1.85 Ga early successor-arc Annabel granite, granodiorite, quartz-diorite and Channing granodiorite plutonic suites. The arc and early successor-arc assemblages are unconformably overlain by sedimentary rocks of the Missi Group. All these rock groups are intruded by the ca. 1.84 Ga late successor arc mafic to ultramafic Boundary- and bimodal Phantom intrusive suites (Fig. 2) (Stern et al., 1999).

The deformation history recorded in outcrops in the Flin Flon exploration camp has been the subject of numerous studies (Stockwell, 1960; Bailes and Syme, 1989; Gale et al., 1998; Lewis et al., 2006; Lafrance et al., *in prep*). Most debate in the literature has focused on grouping generations of fold and fault structures into deformation phases that predate or post-date deposition of the Missi Group. Recent structural analysis and U/Pb zircon geochronology (Rayner, 2010) has yielded new age constraints on the deformation events and provides control on their association with the accretionary, collisional and post-collisional evolutionary stages of the Trans-Hudson orogeny (Lafrance et al., *in prep.*).

Two deformation events (D1 and D2) that predate deposition of the Missi Group have been recorded in rocks of the Flin Flon arc assemblage. The earliest deformation event (D1) can only be locally identified and is represented at the surface by the Burley Lake

faulted syncline (Fig. 2). D2 structures include NNW- to NNE-trending folds (Hidden Lake syncline, Beaver Road- (BRA) and Mandy Road anticlines, (MRA), Fig. 2) that predate 1872 Ma synvolcanic dykes (Rayner, 2010). This age, together with age constraints from the eastern Amisk collage (Lucas et al., 1996; Ryan and Williams, 1999), suggest that D1 and D2 developed during accretionary stages of the Flin Flon Belt ocean floor-island arc deformation history (Lafrance et al., *in prep.*).

Deformation events (D3-D7) that postdate deposition of the Missi Group include N-trending folds (F3) and E-dipping thrust faults (D3) truncated by D4 E-trending brittle-ductile to ductile thrusts. These events imposed a significant regional control on the structural architecture of the mine camp, since the Hook Lake and Flin Flon blocks were thrust over the Missi sedimentary rocks along the NNW-trending D3 Cliff Lake and E-trending D4 Club Lake fault zones, respectively. A regional NW- to NNW-striking shape foliation (S5) and SE-plunging stretching lineation (L5) is persistent throughout the camp and defines the elongation and plunge of the VMS ore lenses. The youngest regional deformation events (D6 and D7) include a regional NE-trending slaty cleavage (S6) that overprints the D5 LS fabric and D7 post-metamorphic subvertical fault zones with reverse and sinistral sense of displacement (Lafrance et al., *in prep.*).

3D MODELLING METHODOLOGY

The knowledge cube spans a volume of 7.5 (northing) by 5 (easting) by 2 (depth) kilometres that intersects the eastern Flin Flon block, the block of unassigned volcanic rocks and western margin of the Hook Lake block (Fig. 2a). This volume was chosen to include the subsurface extent of the VMS-hosting Millrock member and to test a hypothetical cross-section model that structurally links the felsic horizon, hosting the Schist Mandy VMS deposits in the fault block of unassigned volcanic rocks with the Flin Flon-, Callinan- and 777-hosting Millrock member across the SSE-plunging Hidden syncline (Fig. 3).

The surface and subsurface data sources that were used to constrain the model elements of the 3D knowledge cube are listed in Table 1. Lithofacies and lithostratigraphic drill hole logs (provided by HudBay Minerals Inc.), in combination with 2D and 3D seismic interpretations, were used to model the extent of lithostratigraphic contacts (mainly tops) and fault structures. The intersections of these 3D-model elements with the Earth surface were constrained by lithostratigraphic contacts and fault traces extracted from the 1:10 000 scale TGI3 geological map (Simard et al., 2010, Fig. 2a). Mine sections and plans provided additional constraints, for modelling the tops of the Millrock member and the thrust faults that imbricate it, in the vicinity of the mined VMS ore lenses.

The highly heterogeneous spatial distribution of drill holes in the Flin Flon exploration camp reflects the focused exploration and exploitation of the mine horizon. The 3D model elements of the knowledge cube are, accordingly, variably constrained, ranging from 3D-modelled surfaces underpinned by a few, to ones constrained by hundreds of drill holes. Picks from 2D seismic lines and the 3D seismic cube provided complementary constraints, particularly in subsurface volumes with low drill hole density at some distance from the mine horizon.

The degree of variability in constraints can be appreciated in more detail by inspection of Table 2, which lists the number of drill holes and ancillary data sources used for modelling each of the 3D-surfaces. Table 2 also lists 3D model elements that were solely inferred from seismic or surface geological map data and that are, as a result, relatively poorly constrained in their subsurface extent and shape. These elements provided nevertheless valuable additions since they enhance insight in the overall structural architecture of the modelled subsurface or optimize the integral perception of the 3D geological model and TGI3 geological map.

Table 1. Data sources used for 3D geologic modelling of the Flin Flon exploration camp.

Data	Source	Description
Drill hole database	Hudbay Minerals Inc.	581 surface and 2953 subsurface holes with lithology, lithostratigraphy geochemistry, alteration mineralogy, sulphide mineralization and structural log records
Mine sections/plans	Hudbay Minerals Inc.	Interpreted polygons of lithologic units (mostly quartz and quartz-feldspar rhyolite) and 3D surfaces from underground-surveyed (D4) shear zones
3D ore models	Hudbay Minerals Inc.	CAD models of ore lenses from mine surveys
2D seismic sections	GSC- TGI3	IO System IV digital vector accelerometers with a single 3-component sensor. 600-station (1800 channel) symmetric split spread with 5 m sensor spacing
3D seismic cube	Hudbay Minerals Inc.	3775 x 3600m patch, 2800-station (8400 channel); sensor interval 25 m sensor line spacing 200 m; source interval 50 m. – source line spacing 300 m; seismic sources: Vibroseis (30-60 Hz upsweep), dynamite (500 gm in 5 m drillholes) and a 100 cm^3 airgun
Geological map data	TGI3 Flin Flon	1: 10 000 scale cross-boundary geologic map (Simard et al., 2010) strike/dip measurements of structural elements (Lafrance et al., *in prep.*)

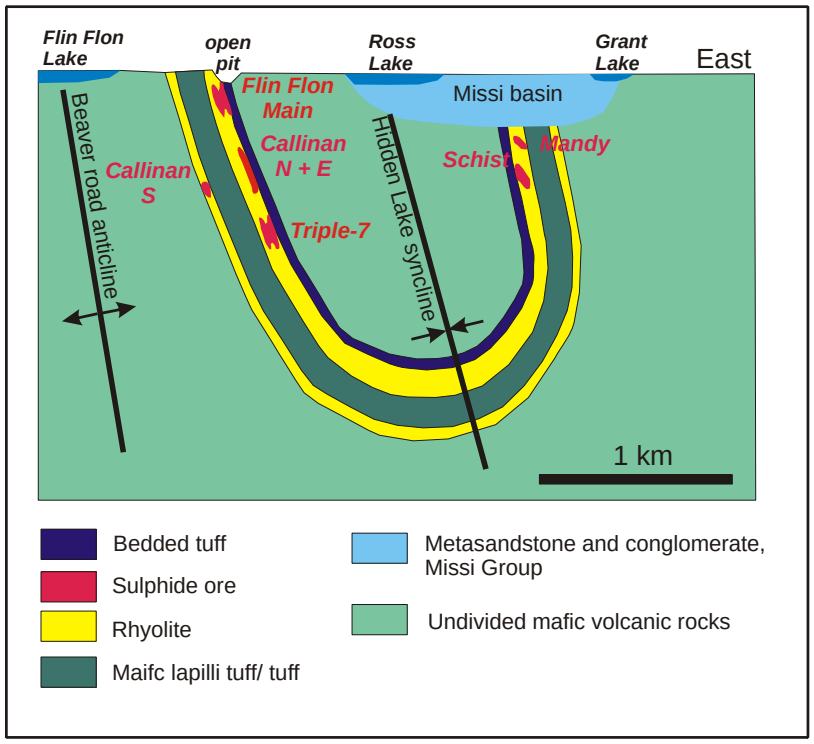

Figure 3. Conceptual structural model depicting the subsurface extent of VMS-hosting units across the Flin Flon exploration camp (modified after unpublished diagram, Hudson Bay Minerals Inc.).

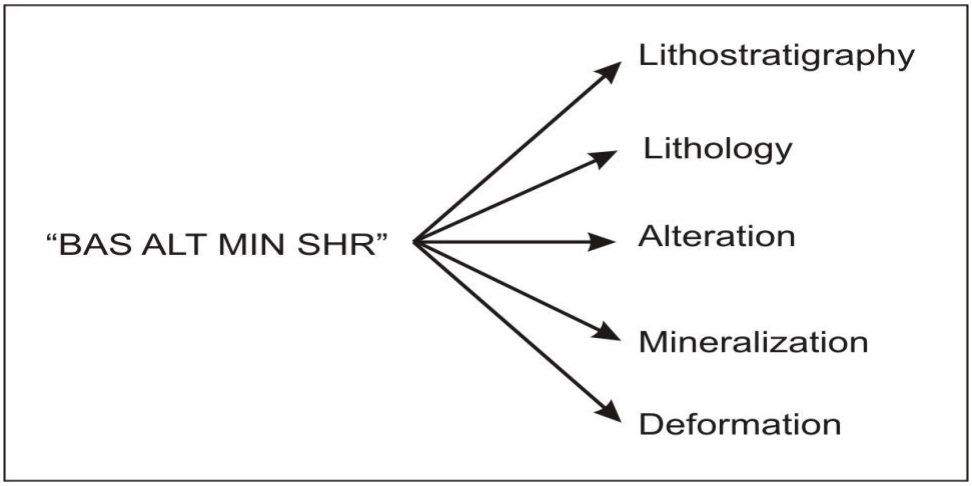

Figure 4. Themes parsed out from industry drill log codes in the normalization of the Flin Flon drill hole database.

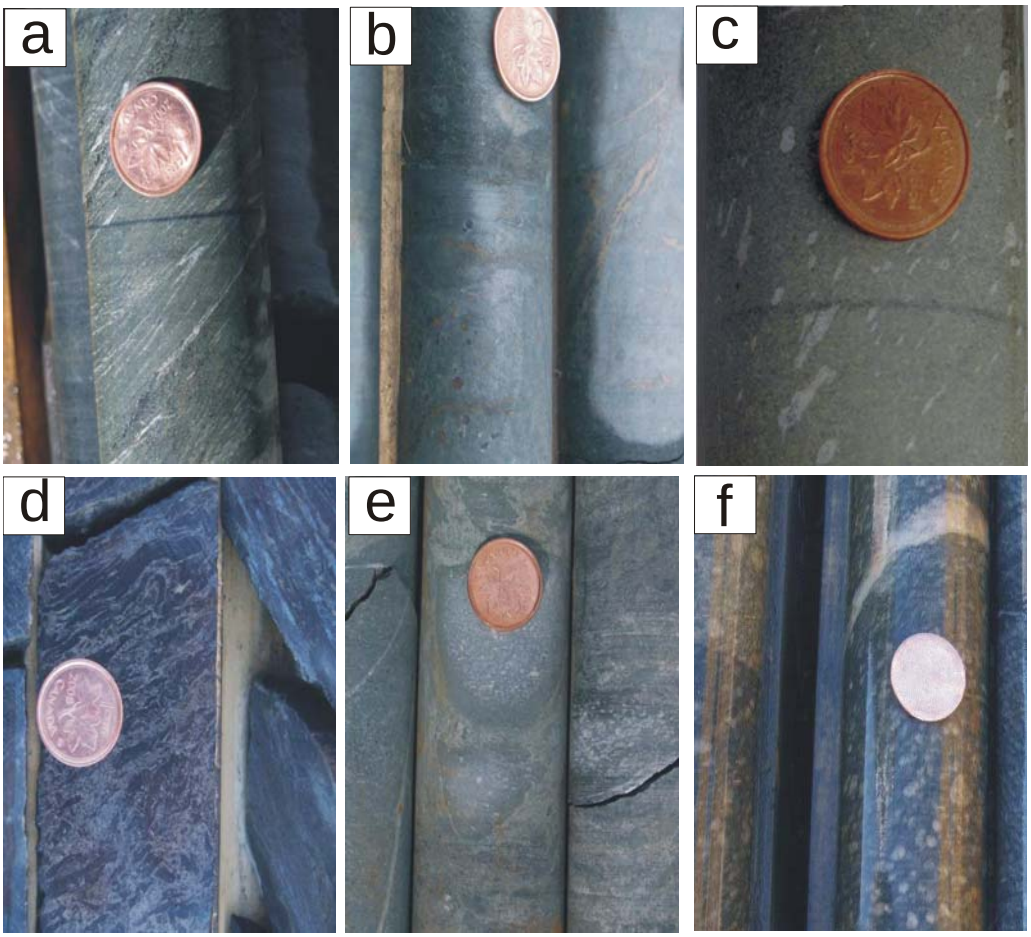

Figure 5. Drill core photographs of diagnostic lithofacies for determining the position of lithostratigraphic units in reference drill holes; (a) Sheared sandstone of the Missi Group deformed in the Club Lake ductile thrust. Note strong planar shape fabric, preferred orientation of quartz-carbonate veins and rootless isoclinal fold; (b) Quartz-phyric rhyolite ('QP' rhyolite) of the Millrock member; (c) amygdaloidal basalt flows of the base of the Hidden formation; (d) Mineralized argillite intercalated in quartz phyric rhyolite (Fig. 5.b). Note alternating sulphide and argillite folded and fragmented bedding; (e) Clast-supported heterolithic tuff breccia ("footwall breccia") of the Millrock member; note rounded scoriaceous clasts. (f) feldspar-crystal tuff matrix-supported fragmentals of the Blue Lagoon member.

Table 2. Drill hole, seismic, geological map and ancillary constraints used for 3D modelling lithostratigraphic contacts, faults and folds. Seismic data constraints include 2D seismic lines ('l1') and the 3D seismic cube ('sc').

3D-modelled surface	Drill hole intersections	TGI3 geological map	Mine sections / plans	2D/3D seismic data	Structural elements
LITHOSTRATIGRAPHIC SURFACE					
TopBlueLagoonL1	**14**	**x**			
TopBlueLagoonL21	**2**		**x**		
TopBlueLagoonL22	**4**				
TopBlueLagoonL23	**2**				
TopBlueLagoonL24	**2**	**x**			
TopMillrockL11	**595**	**x**	**x**	**l1, l2, l3, l7, l8, sc**	
TopMillrockL21	**629**	**x**	**x**	**l1, l2, l3, l8, sc**	
TopMillrockL22	**518**	**x**		**l3, l4, sc**	
TopMillrockL23	**16**	**x**	**x**	**Sc**	
TopHiddenL11	**3**		**x**		
TopHiddenL12	**1**	**x**			
TopHiddenL2		**x**		**l8, sc**	**x**
BaseMissi	**8**	**x**		**l2, l3, l4, l9, sc**	**x**
TopVolcanicImbricate	**14**	**x**		**l2, l3, l6, l9**	
FAULT SURFACE					
TailingsPondFaultUpper					
FlinFlonLake-TailingsPondFaultLower	**6**	**x**			
BasalThrustVolcanicImbricate	**6**	**x**		**l6, l9**	
CliffLakeFault	**1 (4*)**	**x**		**l6, l9**	
ClubLakeFault	**25**	**x**		**l8**	**x**
CatherineFaultLower	**2**	**x**	**x**	**l8**	
CatherineFaultUpper	**2**	**x**	**x**	**l8**	
RailwayFaultLower	**3**	**x**	**x**	**l8**	**x**
RailwayFaultUpper	**6**	**x**	**x**	**l8**	**x**
LakeViewFault	**2**	**x**			
BirchViewFault		**x**			
BlindMissiThrust1				**l9**	
BlindMissiThrust2				**l9**	
BlindMissiThrust3				**l9**	
RossLakeFault		**x**		**l2, l3**	
ChanningFault		**x**		**l2, l3**	
FOLD SURFACE					
FlinFlonCreekSyncline		**x**			**x**
PipeLineSyncline		**x**			**x**
GrantLakeSyncline		**x**			**x**
MudLakeSyncline		**x**			**x**
***constraints located outside knowledge cube**					

Geometric correction

The georeference selected for 3D modelling was UTM, Zone 14N, North American Datum (NAD83), which allowed registering the seismic, drill hole, mine survey and geological map data to a common 3D georeference. The drill hole collar locations, originally registered in mine coordinates ('Callinan metric'), were converted to UTM coordinates by estimating the geometric transformation between the two coordinate systems at eight drill hole collar locations. Table 3 lists the mine and UTM coordinates of eight collars surveyed with differential GPS and the residuals of the estimated transformation. The planimetric (xy) and depth (z) root mean square errors of the 3D transformation are 2.06 and 1.79 m (1 σ) respectively. It should be noted that these error estimates refer to the collar locations and not to the accuracy of the drill hole logs themselves, which are also cumulatively dependent on errors in deviation log readings down the

drill hole. Although the combined collar position and deviation log error has not been estimated, the discrepancies between mine-surveyed ore shells models and ore intersections in the deepest drill holes provided a rough maximum error estimate of 40 m.

Data normalization of descriptive drill hole logs

The drill hole lithology logs were originally coded with a single descriptive field 'rock type' and a sequence of abbreviated characters describing lithology, lithostratigraphy, alteration, deformation and mineralization. These five themes were parsed out by defining SQL (structured query language) queries against the table holding the drill log codes and tables relationally linked to it that cross-reference these codes with classifications defined for each of the themes (Fig. 4). The classification tables were hierarchically structured, which in combination with the parsed out drill log information, facilitated the reclassification and visualization of the five drill log themes on multiple levels of generalization (Table 4). This was essential to support hole-to-hole correlation in search for regional lithostratigraphic markers and would, as well as many other data exploration tasks, not have been feasible without the database normalization effort.

Compilation of lithostratigraphic reference holes

The 1:10 000 scale geological mapping component of the Flin Flon TGI3 project (Simard et al., 2010) accumulated a wealth of lithostratigraphic information that enabled the reconciliation of distinct lithofacies to their recognizable equivalents in drill core. For this purpose a selected set of 52 drill holes were re-logged that, together with 15 previously logged drill holes, provided hundreds of markers for 3D modelling of lithostratigraphic surfaces. Given the 3D distribution of drill holes and diagnostic lithofacies in its core (Fig. 5), three lithostratigraphic markers, from youngest to oldest, were prioritized:

(i) <u>The unconformable/faulted contact with sedimentary rocks of the Missi Group</u>

This marker is easily recognized in drill core by sharp contacts between arkose and conglomerate of the Missi Group and rocks of the Flin Flon arc assemblage or successor arc intrusive rocks. Pebbles, rounded grains and intercalated layers of conglomerate in weakly strained sedimentary rocks with recognizable sedimentary matrix in combination with their higher magnetic susceptibility, allow their easy and unambiguous differentiation from volcanic, volcaniclastic and intrusive rocks in most drill holes. The contact, however, can be difficult to recognize in drill holes that intersect the ductile Club Lake thrust fault, particularly where the contact separates highly altered and sheared rhyolite of the Millrock member from sheared arkose of the Missi Group (Fig. 5a).

(ii) <u>The top of the Millrock member</u>

The contact of the Millrock member with the overlying Hidden formation (Reservoir member, Fig. 2a) has a variable but distinct character in drill core. It is defined by the transition from heterolithic clast-supported mafic volcanic breccia, fine-grained bedded tuff (Railway volcaniclastic rocks of Stockwell 1960), quartz feldspar-phyric rhyolite (Fig. 5b) or ore, to the basal amygdaloidal basalt flows (Reservoir member) of the Hidden formation (Fig. 5c). Intercalations of 20 to 80 cm mineralized bedded and bedding-fragmented argillite (Fig. 5d), previously unknown from outcrop studies, confirm the extrusive origin of quartz feldspar-phyric rhyolite in several drill holes. The contact is frequently intruded by successor arc rocks of the Boundary suite and synvolcanic amphibole-needle phyric basaltic andesite, fine-grained diorite and gabbro intrusions.

Table 3. Ground control points (GCP's) used to compute the geometric transformation between the mine and NAD83, Zone 14 UTM coordinates of eight differential GPS-surveyed drill hole collar locations; dX, dY and dZ are residuals, $RMSE_{XY}$ is the planimetric root mean square error and $RMSE_Z$ is the elevation root mean square error for the least squares estimation of the linear geometric transformation. GCP 7 (RYE09) was excluded from the least squares estimation due to its anomalously high residuals.

GCP	CollarID	X_{mine}	Y_{mine}	Z_{mine}	$X_{utmNAD83}$	$Y_{utmNAD83}$	Z_{NAD83}	dX	dY	dZ
1	FFS042	49687.00	-17125.00	-	314163.39	6075085.92	325.43	-0.76	-0.54	-
2	FFS023	49647.35	-17598.06	-	314102.89	6074613.07	329.60	0.16	0.88	-
3	FFS039	49711.66	-18650.57	2547.71	314123.64	6073558.64	330.93	-0.46	-0.07	0.64
4	FFS038	49871.32	-19690.97	2525.42	314240.65	6072512.95	308.58	-1.47	-1.67	0.57
5	4Q71	51116.15	-19168.54	2525.00	315502.27	6072978.75	330.42	3.39	3.02	2.62
6	FFM001	52884.70	-18919.30	2532.93	317286.67	6073157.47	310.46	-1.98	-0.84	2.87
7	RYE09	51104.80	-20538.57	2545.00	315464.82	6071598.90	346.71	-28.44	11.79	19.12
8	4Q66	51292.23	-18021.67	2532.93	315728.96	6074122.10	315.21	1.11	-0.78	-0.31
	$RMSE_{XY}$ = 2.06 m, $RMSE_Z$ = 1.79 m; average mine datum ($Z_{mine} - Z_{NAD83}$) = 2216.134 m									

Table 4. Hierarchical classification table for encoding drill hole lithology logs (records shown are for felsic igneous rocks). Similar hierarchical classification tables were used to encode lithostratigraphy, alteration mineralogy, sulphide ore mineralogy and deformation logs.

LithoClass1: felsic igneous rock, LithoCode1: FELIGNR					
LithoClass2	LithoCode2	LithoClass3	LithoCode3	LithoClass4	LithoCode4
felsic intrusive	FELINT	Porphyry	QPORPH	feldspar porphyry	FPORPH
felsic intrusive	FELINT	Tonalite	TONAL	tonalite undivided	TONAL
felsic intrusive	FELINT	Granite	GRAN	granite undivided	GRAN
felsic synvolcanic intrusive	FELSINT	rhyolite synvolcanic intrusive	RHYSINT	quartz phyric rhyolite intrusive	RHYINTQ
felsic synvolcanic intrusive	FELSINT	rhyolite synvolcanic intrusive	RHYSINT	rhyolite intrusive	RHYINT
felsic synvolcanic intrusive	FELSINT	rhyolite synvolcanic intrusive	RHYSINT	Magnetite phyric rhyolite intrusive	RHYINTM
felsic synvolcanic intrusive	FELSINT	rhyolite synvolcanic intrusive	RHYSINT	phyric rhyolite intrusive	RHYINTP
felsic synvolcanic intrusive	FELSINT	rhyolite synvolcanic intrusive	RHYSINT	quartz feldspar phyric rhyolite intrusive	RHYINTQF
felsic synvolcanic intrusive	FELSINT	rhyolite synvolcanic intrusive	RHYSINT	aphyric rhyolite intrusive	RHYINTA
felsic synvolcanic intrusive	FELSINT	rhyolite synvolcanic intrusive	RHYSINT	feldspar phyric rhyolite intrusive	RHYINTF
felsic volcanic flow	FELVFL	rhyolite flow breccia	RHYFLB	quartz phyric rhyolite flow breccia	RHYFLBQ
felsic volcanic flow	FELVFL	rhyolite flow breccia	RHYFLB	aphyric rhyolite flow breccia	RHYFLBA
felsic volcanic flow	FELVFL	rhyolite flow breccia	RHYFLB	quartz feldspar phyric rhyolite flow breccia	RHYFLBQF
felsic volcanic flow	FELVFL	rhyolite flow	RHYDFL	Rhyodacite flow undivided	RHYDFLUN
felsic volcanic rock	FELVFL	rhyolite flow	RHYFL	rhyolite undivided	RHYFLUN
felsic volcanic flow	FELVFL	rhyolite flow	RHYFL	phyric rhyolite flow	RHYFLP
felsic volcanic flow	FELVFL	rhyolite flow	RHYFL	quartz feldspar phyric rhyolite flow	RHYFLQF
felsic volcanic flow	FELVFL	rhyolite flow	RHYFL	quartz phyric rhyolite flow	RHYFLQ
felsic volcanic flow	FELVFL	rhyolite flow	RHYFL	aphyric rhyolite flow	RHYFLA
felsic volcanic flow	FELVFL	rhyolite flow	RHYFL	feldspar phyric rhyolite flow	RHYFLF
felsic volcanic flow	FELVFL	rhyolite flow breccia	RHYFLB	rhyolite flow breccia	RHYFLB
felsic volcanic rock	FELVUN	Felsic undivided	RHYUN	felsic volcanic undivided	RHYUN

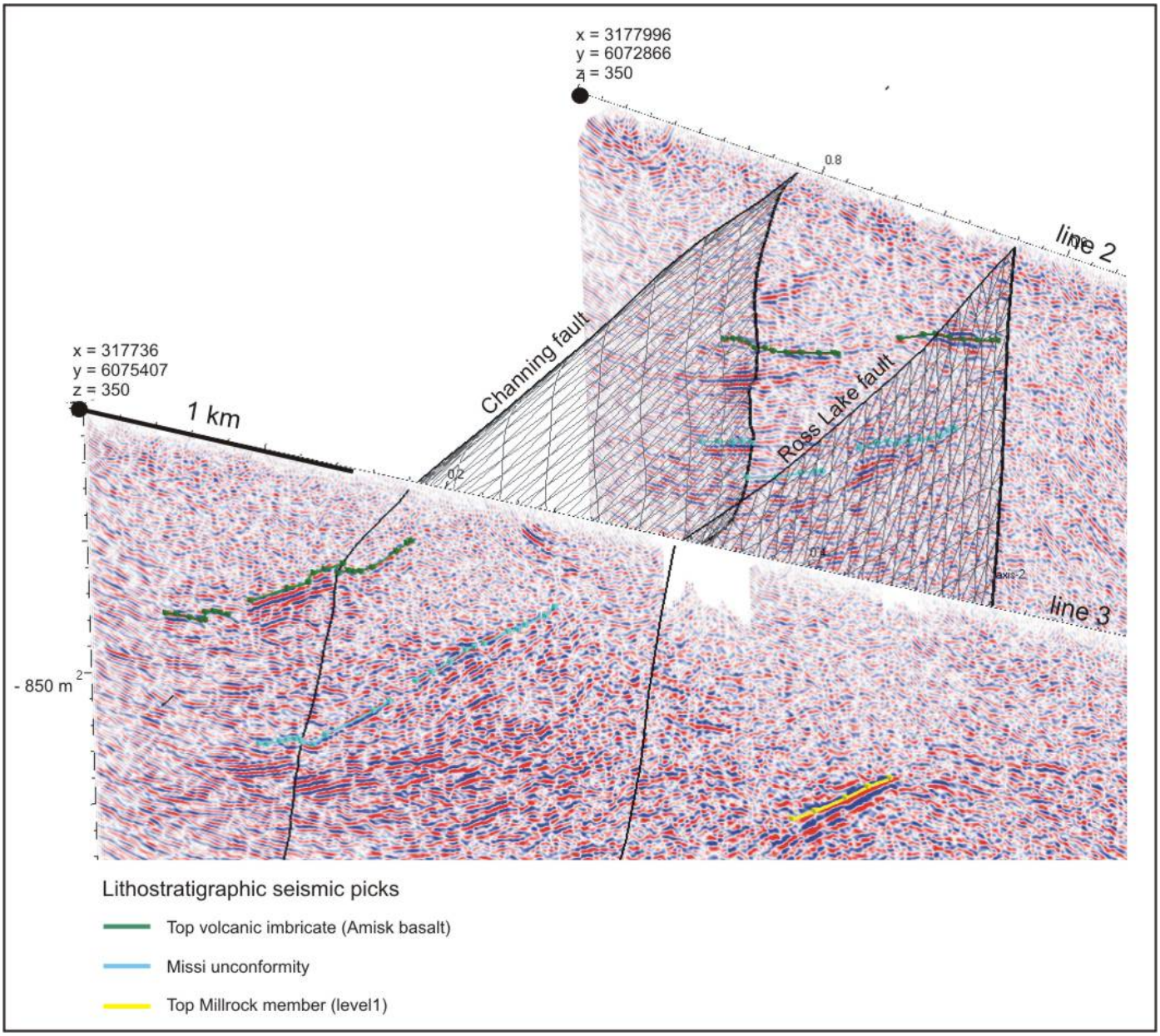

Figure 6. 3D perspective view of seismic line 2 and line 3 with 3D models of the post-metamorphic Channing and Ross Lake faults and lithostratigraphic picks constraining 3D-modelled lithostratigraphic surfaces. Note offset in seismic reflectivity below the Missi unconformity in line 3 suggesting apparent reverse-fault displacement across the Channing fault.

(iii) <u>The top of the Blue Lagoon member</u>

The top of the Blue Lagoon member is recognized in drill core by diffuse to sharp contacts between heterolithic felsic and mafic clast-supported breccias (footwall breccia, Fig. 5e), sparsely-amygdaloidal mafic flows or rhyolite flows of the Millrock member overlying plagioclase crystal-rich basalt tuff and tuff breccia of the Blue Lagoon member (Fig. 5f). This contact is commonly intruded by synvolcanic mafic intrusions, but only rarely by the younger Boundary intrusions. The plagioclase crystal-rich matrix-supported heterolithic breccia of the Blue Lagoon

member is arguably the most diagnostic volcaniclastic rock type recognizable in drill core of the Flin Flon formation. Together with VMS ore lenses and rhyolite with argillite intercalations, they underpin the identification of thrust repeats within the VMS-hosting Millrock member in several drill holes.

A fourth lithostratigraphic contact is represented by the top of a thrust-imbricate of hydrothermally-altered and mineralized basalt and subordinate volcaniclastic rocks identified in fourteen drill holes intersecting the Missi structural basin. This imbricate is aligned down-dip from the "Lakeview showing" (LVS, Fig. 2a). Sheared intervals at its base suggest that the imbricate is in basal fault contact with Missi sedimentary rocks.

Modelling the fault network

A first requisite for 3D geological modelling in any tectonized area is to model the network of faults and shear zones to account for displacements of lithostratigraphic or fault surfaces on opposite sides of the faults that cut them (Renard and Corrioux, 1994). Two fault systems that offset lithostratigraphic units in the Flin Flon exploration camp, of which fault-rock fabrics can be observed in drill core and outcrop, were modelled:

(i) Railway-Catherine-Club ductile D4 shear zones

This comprises a system of S- to SSE-dipping brittle-ductile to ductile thrust faults established by detailed surface (Stockwell, 1960) and underground mapping (Tessier and O'Donnell, 2001) that include from north to south the Club Lake, Lower Catherine, Upper Catherine, Lower Railway and Upper Railway faults. The Catherine and Railway faults sole into the basal, listric S-dipping ductile Club Lake shear zone that has brought up Amisk collage rocks over Missi Group sedimentary rocks. These two to five-meter wide shear zone splays in the hanging wall of the Club Lake thrust fault imbricated the mine horizon on at least three structural levels.

(ii) Post-metamorphic D7 subvertical faults

This comprises a system of subvertical ductile to brittle post-metamorphic fault zones, including the Ross Lake and Channing faults. The faults have potentially a long history of reactivation. Evidence for their late activity is manifest in offsets of all earlier fabrics and metamorphic isograds (Gale et al., 1998 and references therein). The faults also offset the unconformity between the Flin Flon arc assemblage and Missi Group with lateral and vertical components of displacement (Fig. 2a).

The Railway, Catherine and Club Lake faults were modelled by fitting surfaces to constraints from underground mine surveys, faults traces extracted from the TGI3 geological map and seismic interpretations of fault tips using the gOcad™ DSI (Discrete Smooth Interpolation) routine (Mallet, 1992).

The Club Lake structure was modelled by fitting surfaces to 25 drill-intersected Amisk collage-Missi Group contacts, its mapped surface trace and seismic picks from line 8. Since Amisk basement-Missi Group contacts are intersected at different structural levels in adjacent drill holes, the Club Lake fault could not be fitted to a single surface. As a result, the fault was modelled as a multi-segmented structure consisting of ramp and flat segments coinciding with distinct seismic reflectors on line 8. The Catherine and Railway faults were modelled by fitting surfaces to four mine-surveyed faults established in the 777 and Callinan mine workings. Strike and dip measurements of shear zone fabrics collected in outcrops at surface and the overall attitude of seismic reflections on line 8 provided additional constraints to link the mine-surveyed fault segments with their corresponding surface traces.

The subvertical to steeply E-dipping Ross Lake and Channing faults were modelled by fitting surfaces to

aligned discontinuities and truncated seismic reflectors and their mapped surface trace (Fig. 6) and a drill hole with a 4 m quartz-carbonate veined cataclasite interval of the Ross Lake fault intersected at a depth of 60 m. The modelling of these faults is somewhat tentative, since there are multiple solutions in tracing them to depth between the truncated seismic reflectors.

An early system of E-dipping and N-trending thrust faults that includes the Flin Flon Lake, Lower and Upper Tailings Pond faults (Fig. 2a) is not evidently exhibited as demonstrable fault contacts or shear fabrics in drill core, but rather inferred from: (i) repeated lithostratigraphy, (ii) repeated VMS ore lenses and, (iii) repeated rhyolite intervals that contain an intercalated argillite horizon. Since older units are consistently in hanging wall relationship with younger units in both outcrop and drill core, thrust faulting provides the most favourable explanation for the repetition of the VMS-hosting Millrock member (as opposed to a stratigraphic repetition). The thrust faults truncate D2 folds (Fig. 2a) and are tentatively grouped with similarly oriented E-dipping and N-trending D3 thrusts that postdate deposition of the Missi Group established in drill hole and outcrop studies further east (Lafrance et al., *in prep.*). It can not be ruled out, however, that the N-trending thrust-imbrication of the Millrock member initiated earlier, perhaps coevally with the development of the NNW-trending D1 Burley Lake faulted syncline.

The first of the two N-trending thrust faults east of the Hidden Lake syncline was established at the base of the E-dipping volcanic imbricate where mafic basalt flows are in sharp hanging wall fault contact with Missi sedimentary rocks. The second thrust corresponds to the Cliff Lake fault (Fig. 2a). This E-dipping structure was modelled from its intersection in five drill holes and its mapped surface trace. More study is required to unravel the kinematic history of the Cliff Lake fault since kinematic evidence established in outcrop indicates both dextral and sinistral transcurrent displacement (Kremer and Simard, 2007), an inference more consistent with the kinematics of the post-metamorphic D7 faults. Since, however, the five drill holes show that the Hook Lake block was brought up for at least 1 km over sedimentary rock of the Missi Group, D7 strike-slip faulting may have reworked an older D3 thrust fault.

Modelling lithostratigraphic surfaces

The success of 3D modelling lithostratigraphic surfaces largely depends on drill hole density, the quality and consistency of associated log descriptions, and, the extent to which unique lithostratigraphic markers are present and can be recognized in drill core (Schetselaar et al., 2010). As previously described, such markers were successfully established by re-logging drill core, and together with the seismic data, provided the principal constraints for 3D modelling the tops of lithostratigraphic units in the subsurface.

The gOcad Sparse^{TM} plug-in (Sprague and de Kemp, 2005) was used for modelling the tops of the Millrock member on 14 parallel sections spaced 479 m apart and dipping 54^{o} towards the northwest. A 'volume of interest' (voxet) was defined around the mapped contacts and drill hole intervals that constrain the 3D location of the Millrock member. The voxet longest axis defined the projection axis and was chosen parallel to the plunge of the regional stretching lineation to minimize geometrical distortions and cross-overs in the projection of geological constraints. The maximum distance at which geological constraints were projected on the sections amounted to 250 m.

The projected elements included intervals from the lithostratigraphic reference drill holes, generalized lithofacies drill hole intervals, modelled faults and geological contacts extracted from the Flin Flon TGI3 geological map (Simard et al., 2010). Curves representing the top of the Millrock member were digitized on the sections honouring the projections of sparsely distributed stratigraphic markers from the lithostratigraphic reference drill holes and the densely distributed projections of lithofacies transitions (*e.g.* from rhyolite, sulphide ore or bedded tuff to

basalt flows) that mark the contact between the Millrock member with the overlying Hidden formation. The interpreted curves were subsequently interpolated to 3D surfaces using NURBS (Non-Uniform-Rational-B-Spline) interpolation routines (Farin, 1988). Lastly, topological relationships between the 3D-modelled tops of the mine horizon and the fault network were established to model fault displacements.

The tops of the Blue Lagoon member, Hidden formation, Missi basal unconformity, and thrust-imbricate of mafic volcanic rocks were directly modelled via DSI interpolation routines by fitting surfaces to the relatively few drill hole intersections and seismic picks that constrain them (Table 2).

Modelling fold structures

As opposed to F1 and F2 folds that were predominantly established by mapping opposing facing directions in basalt flows of the Flin Flon arc assemblage, F3 and F4 folds in the Missi Group are defined by regionally traceable lithostratigraphic markers. Conglomerate beds at different stratigraphic levels in the Missi Group outline F3 and F4 fold structures that have been extensively documented in previous structural studies (Stauffer and Mukherjee, 1971; Bailes and Syme, 1989; Gale et al., 1998; Lafrance et al., *in prep.*). Although none of these fold structures are intersected in drill holes, their 3D geometry was modelled by using structural projection techniques similar to those described for modelling the Millrock member.

Figure 7 shows the map outline of the tops of conglomerate beds and bedding elements of the Flin Flon Creek, Pipe Line, Grant Lake and Mud Lake synclines. The hinge lines of these folds were defined by fitting best-fit great circles through poles to bedding in six structural domains (Fig. 7). The folded outline of the conglomerate markers were digitized on sets of parallel sections normal to these hinge lines using the projected map contacts and bedding elements to guide the interpretation. Subsequently, the digitized curve sets were interpolated to 3D form surfaces using NURBS interpolation routines. The F4 Flin Flon Creek and F3 Grant Lake synclines were the easiest to model since they are cylindrical structures defined by single girdle distributions. The Mud Lake and Pipe Line synclines, however, are doubly plunging F3F4 fold interference structures (Fig. 7) (Lafrance et al., *in prep.*). These non-cylindrical fold interference structures were modelled by digitizing curves on two sets of parallel sections, each oriented normal to the hinge lines of their corresponding structural domain. The 3D fold form surfaces were modelled by: (i) fitting form surfaces to curve sets after merging them from both structural domains (Mud Lake syncline) or (ii) iteratively fitting the form surfaces to each curve set by sequencing NURBS and DSI interpolation routines (Pipe Line syncline).

Model refinement and validation

Several methods were employed to validate or refine the 3D-modelled lithostratigraphic, fold and fault surfaces. Unit outlines from mine sections and plans, drill hole lithofacies intervals and 3D ore shell models provided secondary constraints for fine tuning the geometry of the tops of the Millrock member that are defined for much of their surface area by rhyolite flows and massive sulphide ore. Additional lithostratigraphic classifications of lithology logs that were not physically re-examined contributed to a similar purpose and refined the geometry of the 3D-modelled tops of the Blue Lagoon member.

Seismic ray-tracing techniques were employed to validate 3D-modelled lithostratigraphic and fault surfaces constrained by a limited number of drill holes, which included 3D-modelled surfaces of the volcanic imbricate, the Missi unconformity, and the Catherine and Railway faults. These 3D-modelled surfaces were iteratively adapted by assessing and minimizing discrepancies between their ray-traced projections and corresponding reflectors on 2D seismic sections (Fig. 8; Malinowski et al., *in prep.*).

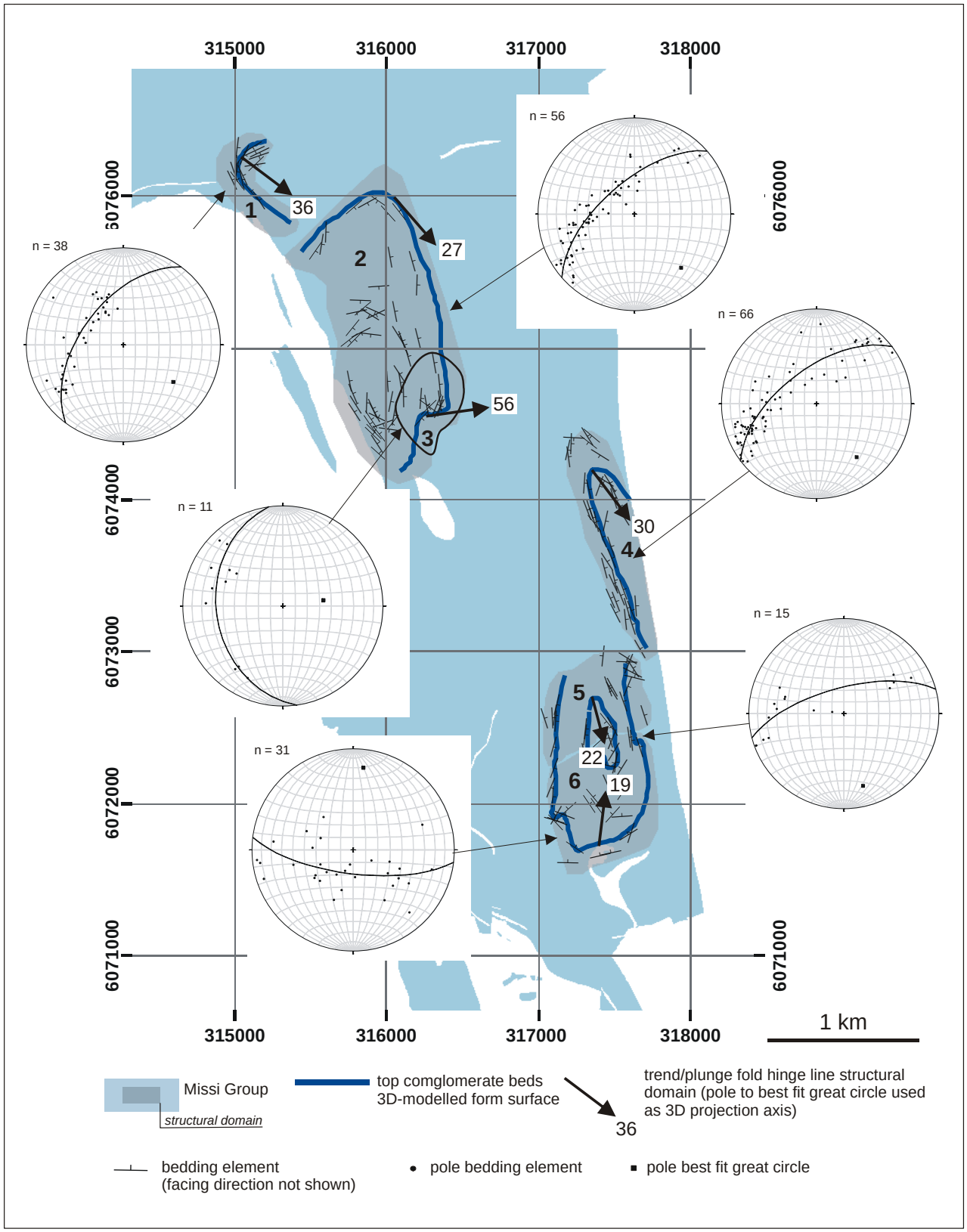

Figure 7. Stereographic projection analysis of bedding elements (data courtesy Bruno Lafrance) for 3D modelling fold structures in the Missi structural basin. Hinge lines derived from best-fit great circles for the bedding elements of distinct structural domains (numbered polygons) defined projection axes to model fold structures in conglomerate beds at different stratigraphic levels in the Missi Group.

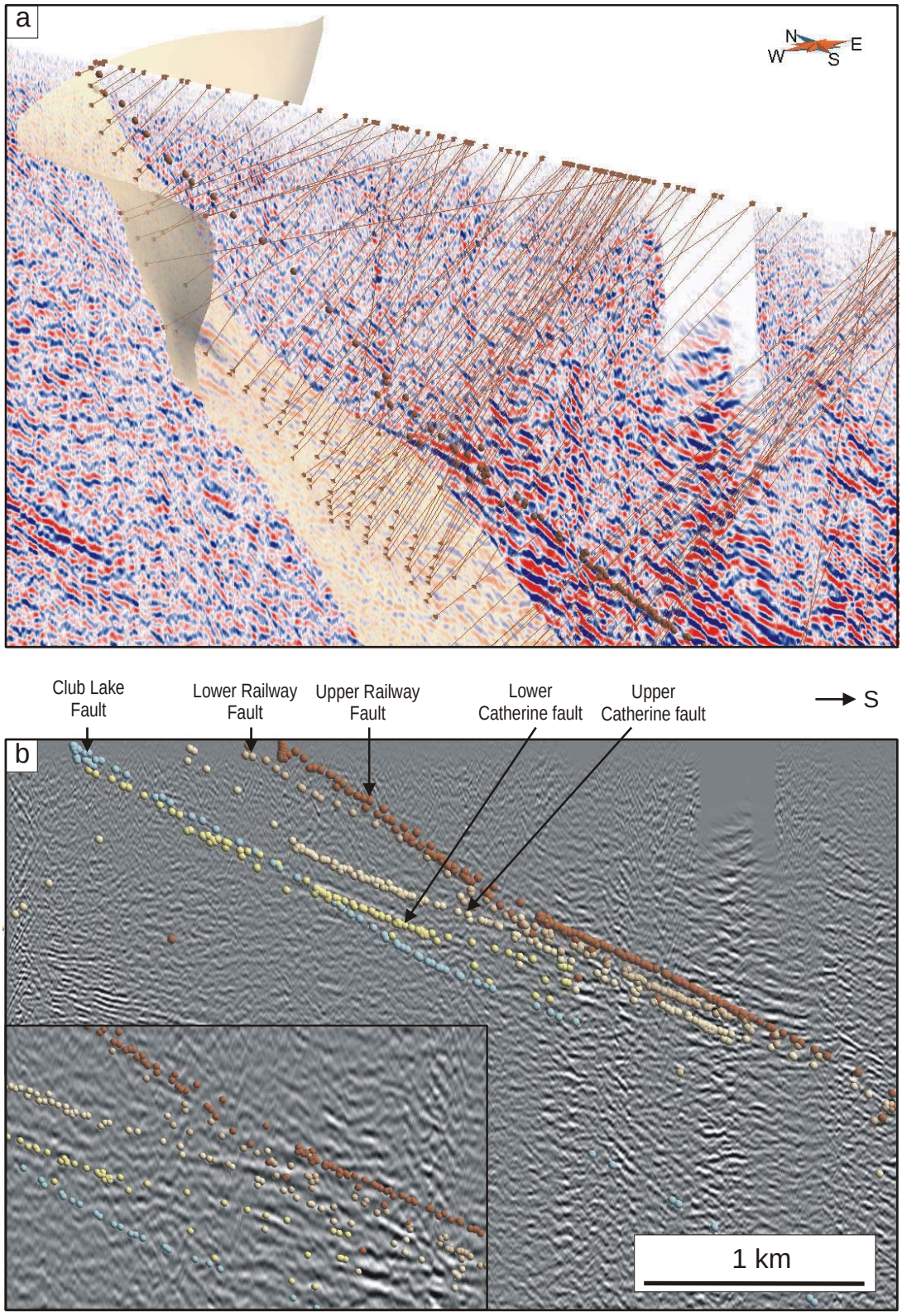

Figure 8. Seismic ray tracing results for **v**alidating the 3D-modelled Club Lake, Catherine and Railway fault surfaces. a) 3D perspective view of Lower Railway fault model and line 8 (unmigrated). Cubes show reflection and receiver position of simulated seismic rays with connecting lines representing the ray paths; spheres show vertically projected reflections below receiver positions; b) Line 8 (unmigrated) with superimposed 2D reflection positions. Inset shows detailed view of a part of Fig. 8b.

MODEL DESCRIPTION

The following sections describe the 3D-modelled lithostratigraphic, fold and fault surfaces of the 3D Flin Flon knowledge cube in order of structural position and deformation history. Grouped and individual model elements are specified in italic fonts within square brackets to aid cross-referencing the description with the 3D model available for user-interaction (3DModel). In addition, Figure 9 shows a fence diagram with intersections of the true geometry of the 3D-modelled surfaces on two perpendicular cross-sections, which provides a synthesized view of the general 3D architecture of the Flin Flon exploration camp. Basic instructions for interacting with the 3D model are provided in Appendix 1.

3D Lithostratigraphic surfaces

Top of the Blue Lagoon member
[STRAT1TopBlueLagoon]

The Blue Lagoon member is the oldest unit of the Flin Flon formation represented in the 3D knowledge cube. The contact of the Blue Lagoon member with the overlying Millrock member is due to its diagnostic plagioclase crystal fragment-bearing volcaniclastic lithofacies established with a high degree of certainty. The sparseness of drilling at these structural levels, however, limits the modelling of its full lateral extent.

The Blue Lagoon member has been stacked on two regional structural levels *[TopBlueLagoonL1, TopBlueLagoonL2*]* in the footwall and hanging wall of the N-striking Flin Flon Lake and Lower Tailings Pond fault array *[FlinFlonLakeTailingsPond-FaultLower]*. The upper panel has been imbricated by the Upper Tailings Pond fault *[TailingsPond-FaultUpper]* and has been brought up over a locally-defined imbricate of the Hidden formation *[TopHiddenL11]*. The upper panel was re-imbricated by the Catherine and Railway faults *[Catherine-FaultLower, CatherineFaultUpper, RailwayFault-Lower, RailwayFaultUpper]* resulting in a total of four imbricates at the upper structural level: *[TopBlueLagoonL21, TopBlueLagoonL22, TopBlue-LagoonL23, TopBlue-LagoonL24]*.

Top of the Millrock member
[STRAT2TopMillrock]

The Millrock member also exhibits regional-scale duplications interpreted to result from W-vergent thrust faulting (Fig. 9). This interpretation is corroborated by repeated N-striking lithostratigraphic units in reference drill holes and the -740 m mine plan in the vicinity of the 777 deposit *[MinePlan]* and at surface by N-trending repetitions of Millrock units north of the Tailings Pond and south of the South Main mine shaft (Fig. 2a). Four top surfaces of the Millrock member were established by 3D lithostratigraphic modelling, including the tops of two regionally-defined thrust panels *[TopMillrockL1, Top-MillrockL21]* and two imbricates in the northern strike-extent of the upper panel in the footwall of the Railway *[TopMillrockL22]* and Catherine faults *[TopMillrockL23]*. The modelled enveloping surfaces dip moderately towards east with dip angles ranging from 50^{o} to 60^{o}. Locally, however, the range in dip angles decrease to 20^{o} to 30^{o} at depth, where sigmoidal patterns in the 3D-surfaces model deflections induced by non-coaxial ductile deformation accommodated by the S- to SSE-dipping Catherine and Railway thrust faults.

Seismic reflectors on in-line (E-W) sections of the 3D seismic cube suggest that the Millrock member thrust panels retain their eastern dip attitude beyond the depth range of drilling (Fig. 10). These seismic reflectors continue east of the Ross Lake fault underneath the Missi structural basin, where their persistent eastern dip attitude is unconformable with the hinge zone of the Hidden Lake syncline above it (Fig. 9).

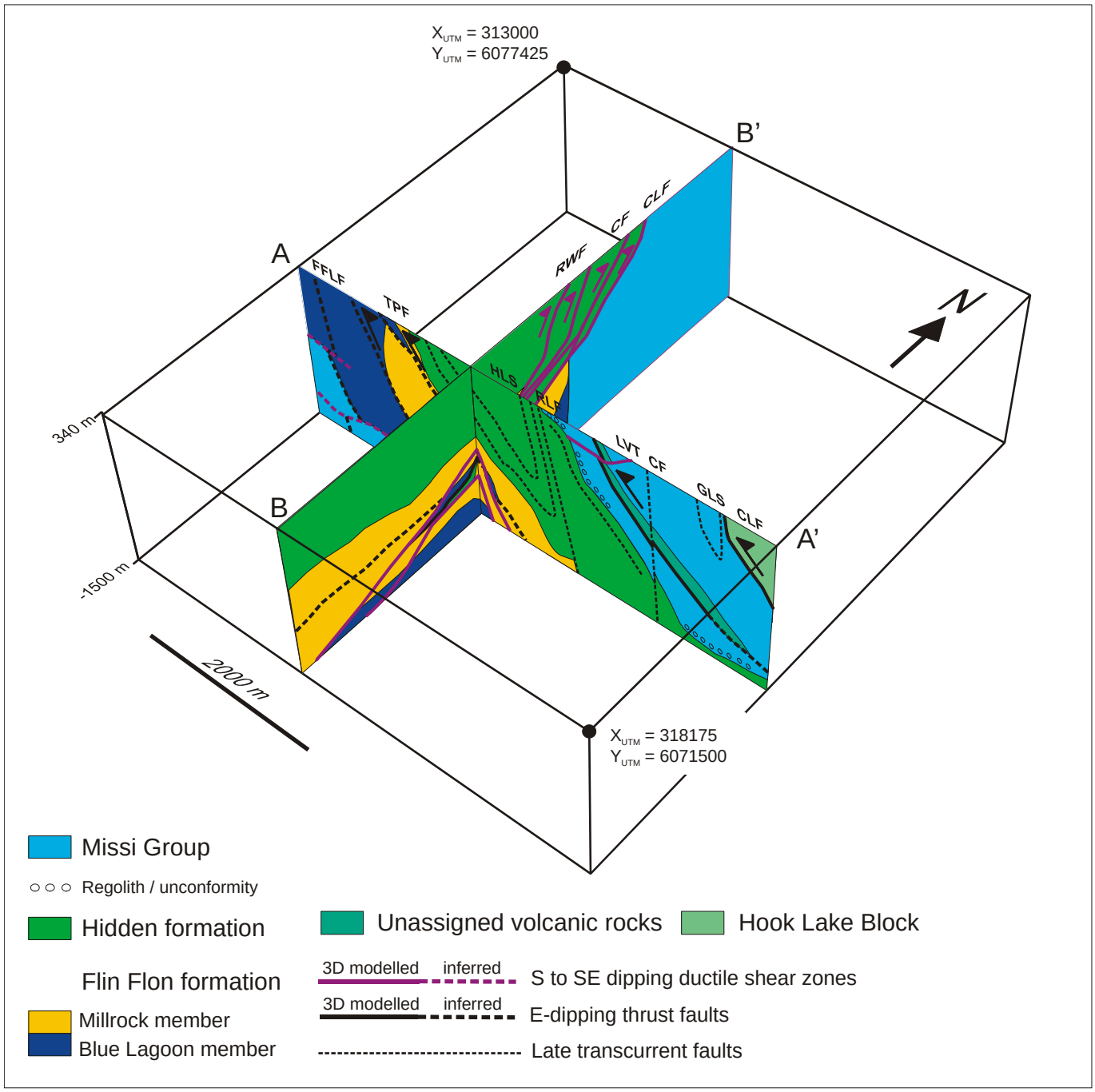

Figure 9. 3D block diagram of the Flin Flon exploration camp showing modelled and inferred lithostratigraphic units and faults on E-W and N-S sections. CLF=Club Lake fault, CF=Catherine fault (Upper), RWF=Railway faults, FFF=Flin Flon Lake fault, TPF=Tailings Pond fault, LVT=Lake View thrust, CF=Channing fault, CLF=Cliff Lake fault, HLS= Hidden Lake syncline, GLS=Grant Lake syncline.

3DModel. 3D interactive model (click on figure to activate) of the Flin Flon exploration camp containing 3D-modelled lithostratigraphic, fold and fault surfaces, lithostratigraphic reference drill holes, the generalized TGI3 geological map, ancillary underpinning data: -740 mine plan, VMS ore shells (777 excluded), outlines of QP rhyolite from mine sections and plans, map layers: hydrography, 2D topography (provincial border, roads, railways), 3D topography (mine shaft and Flin Flon stack). See Appendix 1 for basic instructions on how to interact with the 3D model.

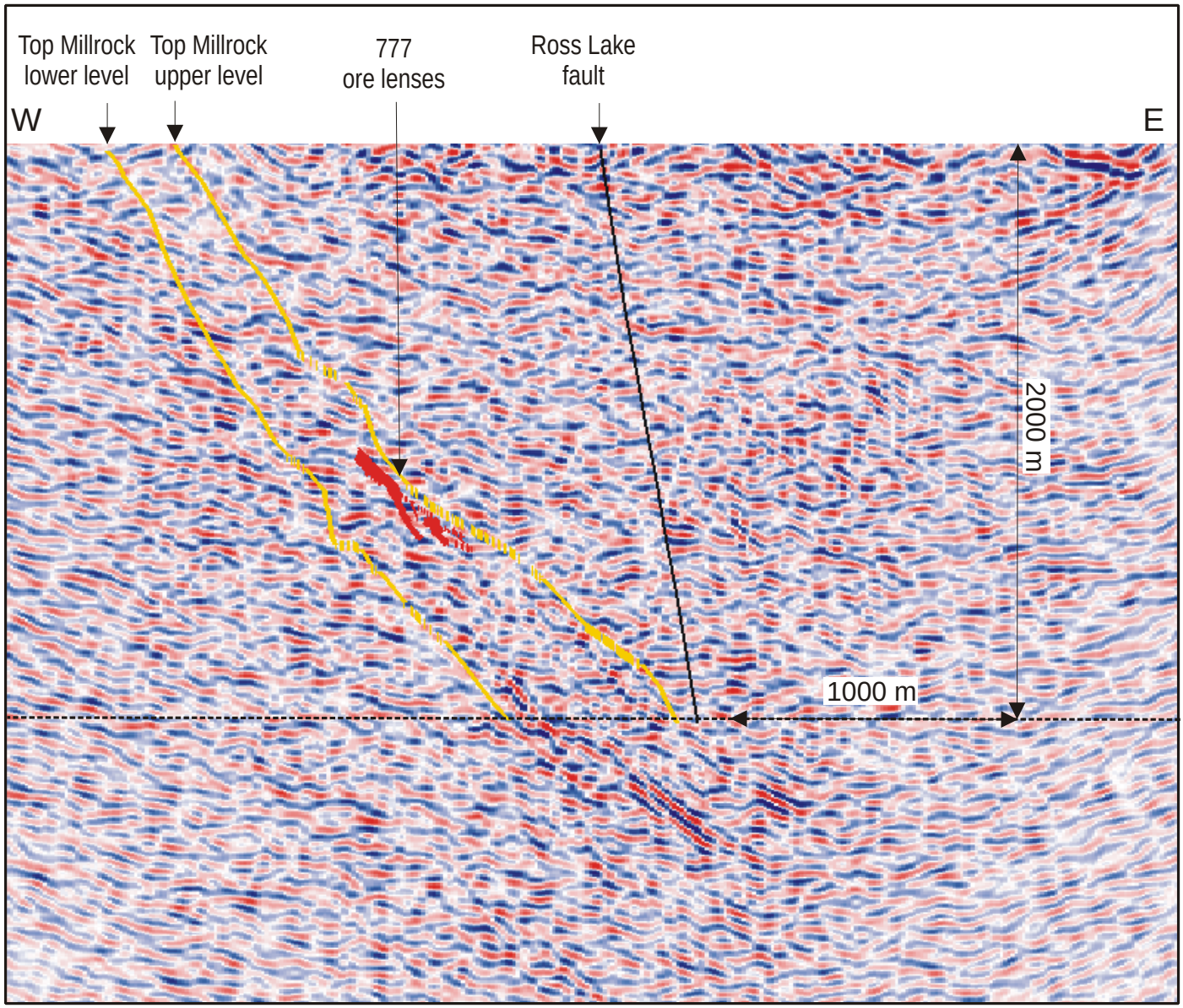

Figure 10. In line 125 (E-W) of the 3D seismic cube with intersection of 3D model elements superimposed. Note E-dipping reflectivity in the down-dip extent of the Millrock top surfaces on both sides of the Ross Lake fault below the 2 km depth range.

Further west towards the Flin Flon Main deposit, the N-trending tectonic repetition is less obvious, since repeats in distinct lithostratigraphic intervals are lacking. Instead, 200 m thick intervals of coherent rhyolite are intersected. These anomalously thick rhyolite intervals may, however, be the result of internal layer-parallel thrust stacking as locally observed in recently drilled Millrock intervals in the footwall of the 777 VMS deposit. Moreover quartzo-feldspathic mylonite observed in a thin section of rhyolite intersected in a drill hole 20 m above the Club Lake fault, previously logged as fine-grained rhyolite overlain by a 8 m thick interval of sheared volcaniclastic rocks, suggests that seemingly homogeneous undeformed intervals of rhyolite may be cut by shear zones of significant width.

The upper level imbricates of the mine horizon in the footwall of the Lower Railway and Catherine faults are truncated by the Club Lake fault further north *[ClubLakeFault]*. The 3D-modelled Millrock surface *[TopMillrockL22]* between the Upper Catherine and Lower Railway faults portrays an isoclinal fold plunging subparallel to the SE-plunging stretching lineation recorded in these shear zones at surface (Lafrance et al., *in prep.*). The shape and orientation of this fold structure are conformable to a closely-spaced duplication of Callinan ore lenses *[ORECallinanEastZone, Lens: 1, 2, 3, 5]* and suggest that this structure is a sheath fold formed during NW-directed movement along the Upper Catherine fault.

Top of the Hidden formation [STRAT3TopHidden]

Due to limited subsurface constraints the 3D-modelled surface representing the contact between the Hidden and Louis formations is tentatively being inferred from its mapped surface trace, the general attitude of the underlying members of the Flin Flon formation and seismic picks from line 8 (Fig. 11). Although this moderately E-dipping surface of the western limb of the Hidden Lake syncline *[TopHiddenL2]* is poorly constrained in comparison to all the other lithostratigraphic surfaces, it was added to the 3D knowledge cube to facilitate the correlation of TGI3 geologic map patterns with the 3D model elements.

The tops of two imbricates from the Hidden formation *[TopHiddenL11, TopHiddenL12]* in the footwall of the VMS ore system were modelled using constraints from lithostratigraphic reference holes, surface contacts and the -740 m (MSL) mine plan near the 777 mine workings. These surfaces represent the tops of imbricates in footwall fault contact with the Millrock and/or Blue Lagoon members that developed, as previously mentioned, during D3 thrust faulting. The geometry of these imbricates, in addition to being constrained by drill holes, mapped contacts and mine plans, were modelled to be conformable to the densely-constrained Millrock surfaces in their vicinity. The N-trending thrust-imbricate *[TopHiddenL11]* was overthrusted by the Millrock member *[Top-MillrockL21]* along the Railway faults (Fig. 9).

Base of the Missi Group (regolith, basal unconformity) [STRAT4BaseMissi]

The basal unconformity *[BaseMissi]* between the Flin Flon volcanic arc-early successor arc basement and sedimentary rocks of the Missi Group has been modelled from eight drill holes and numerous picks from the 3D seismic cube and 2D seismic sections. The 3D-modelled surface outlines a N-trending asymmetric structural depression with steeply E-dipping possibly fault-controlled ramps west of the Channing fault and subhorizontal dip attitudes east of it. Along N-S sections, east of the Channing fault, the attitude of the unconformity changes from steeply N-dipping at its E-trending exposure in the south to shallowly N-dipping to subhorizontal attitudes in the subsurface further north. Local dip reversals towards south can be observed in the hanging walls of blind D4 thrust faults *[THRUSTEastTrendD4:BlindMissi-Thrust]* that were inferred from the interpretation of 2D seismic lines (Malinowski et al., *in prep.*) and the abrupt truncation of the volcanic thrust-imbricate in adjacent drill holes. The overall 3D geometry of the contact is conformable with the map patterns and 3D models of synclines in the Missi structural basin *[FOLDF3F4MissiConglomerate: GrantLakeSyncline, MudLakeSyncline, PipeLineSyncline]* and N-trending thrust faults *[BasalThrustVolcanicImbricate, CliffLakeFault]* suggesting that the geometry of the Missi structural basin is dominantly controlled by N-trending D3 and E-trending D4 folds and thrust faults.

Top of intra-Missi volcanic imbricate [STRATUTopVolcanicImbricate]

Intersections of mafic volcanic with minor volcaniclastic rocks from fourteen drill holes define a moderately E-dipping partly blind thrust-imbricate *[TopVolcanicImbricate]* in footwall fault- and hanging wall stratigraphic contact with sedimentary rocks of the Missi Group. This imbricate is also constrained by

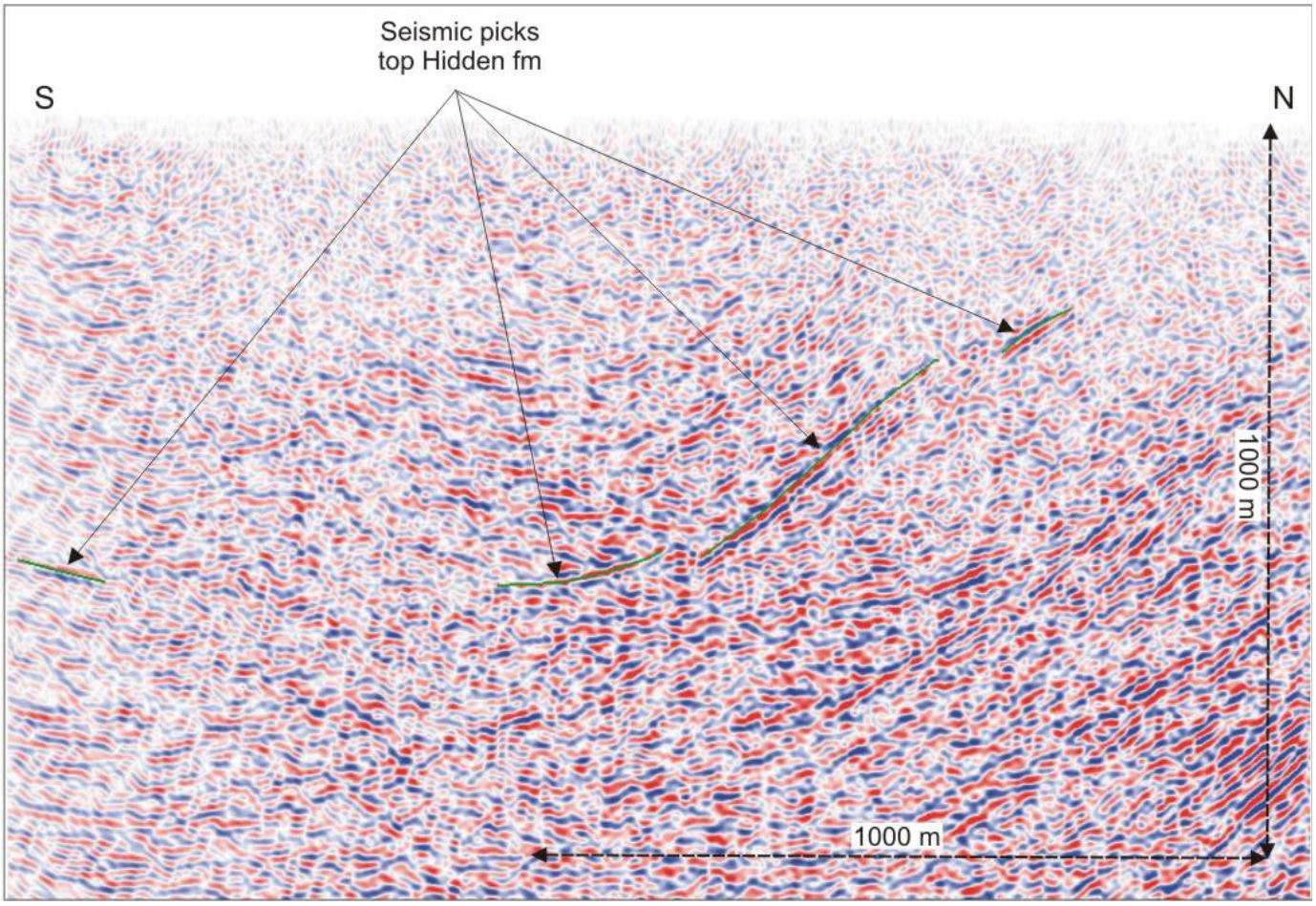

Figure 11. Migrated 2D seismic survey line 8 with seismic picks for modelling the normal stratigraphic contact between the Hidden and Louis formations.

E- and ENE-dipping seismic reflectors on lines 2, 3, 6 and 9 (Table 2). The imbricate is locally exposed within the Missi structural basin as a lensoid unit defined by NNW and ESE-trending thrust faults on its western and northern limits and by an unconformable contact with Missi Group sedimentary rocks on its eastern limit (Fig. 2a).

Drill holes east of the Channing fault intersect a single continuous interval of mafic volcanic rocks. Multiple parallel seismic reflectors on line 9 and drill holes at the Lakeview showing, however, suggest that the interval consists of multiple smaller-scale imbrications (Malinowski et al., *in prep.*). Although its extent beyond the 2D seismic lines and drill holes remains uncertain, the imbricate seems to project down-dip in the footwall of the Cliff Lake fault.

3D fault surfaces

North-trending D1(?)-D3 thrusts
[THRUST1NorthTrendD1D3]

Four N-trending, E-dipping thrust faults were modelled that were established by surface mapping (Simard et al., 2010) and recognition of repeated lithostratigraphic units in drill holes. The thrust faults either imbricated rocks of the Flin Flon arc assemblage internally or with Missi Group sedimentary rocks and accommodated significant tectonic transport in westerly directions.

Two moderately E-dipping thrust faults *[TailingsPondFaultUpper, FlinFlonLakeTailings-PondFaultLower]* were modelled to explain repeated

lithostratigraphic units in the Flin Flon formation. Both surface mapping (Lafrance et al., *in prep.*; Simard et al., 2010) and 3D subsurface modelling demonstrate that these thrust faults are developed along or parallel to N-trending lithostratigraphic contacts that predate D4 shear zones. Locally, however, they imbricated underlying and overlying lithostratigraphic units, which resulted in the local stacking of Blue Lagoon member and basal Hidden formation imbricates between the lower and upper Millrock member thrust panels (Fig. 9).

Assuming that the duplicated Millrock member formed once a single continuous lithostratigraphic interval, its displacement along the E-dipping N-trending thrust faults must have been significant. Without considering the effects of erosion, the restoration of the upper Millrock member panel with the lower Millrock member panel along the Upper Tailings Pond fault, requires a minimum displacement of 1.5 km (Fig. 9). Although more work is required to corroborate this tentative kinematic interpretation, it would imply that the relatively small breccia sulphide lenses of the South Callinan ore zone *[ORECallinanSouthZone]* represent the western lateral equivalent of the East Callinan breccia ore zone *[ORECallinanEastZone]*.

Two post-Missi moderately E-dipping thrust faults that transported Flin Flon arc assemblage rocks over sedimentary rocks of the Missi Group are located east of the Ross Lake fault. These include the thrust fault at the base of the imbricate of hydrothermally-altered basalt *[BasalThrustVolcanicImbricate]* and the NNW-trending moderately E-dipping Cliff Lake fault *[CliffLakeFault],* (Fig. 2a).

The Cliff Lake fault was previously interpreted along its southern strike extent, as a steeply E-dipping post-collisional fault (Lucas et al., 1995). Its 3D-modelled dip, as well as the geometry of the basal thrust fault, however, is concordant to E-dipping bundles of seismic reflectors on Lithoprobe line 5 (Geological Survey of Canada) suggesting that these structures represent earlier thrust faults that define the base of regionally E-dipping thrust-imbricates of Missi Group sedimentary and Flin Flon arc assemblage rocks (Fig. 12).

East-trending D4 thrusts
[THRUSTEastTrendD4]

The 3D models of the Club Lake, Catherine and Railway faults *[ClubLakeFault, CatherineFaultLower, CatherineFaulUpper, RailwayFaultLower, Railway-FaultUpper]* represent a coherent listric system of S- to SSE-dipping brittle-ductile to ductile shear zones. This system, of which the Club Lake shear zone forms the basal splay, steeply cuts the Hidden formation in the hanging wall with dip angles ranging from 50^{o} to 80^{o}. The dip angles of the splays decrease to 20^{o} - 30^{o} and converge with each other in the footwall of the VMS deposits where the high strain zones separate Millrock member imbricates and are localized in hydrothermal alteration zones rich in chlorite, sericite and talc.

Important topological insight in the thrust imbrication of the Millrock member can be obtained by analyzing the spatial relationships between 3D-modelled Millrock lithostratigraphic and fault surfaces. Figure 13 shows a 3D model of the upper and lower tops of the Millrock member and the Railway, Catherine and Club Lake faults. The D4 shear zones cut through both the lower and upper Millrock imbricates, suggesting that the N-trending regional thrust repetition of the mine horizon must have predated the local N-vergent imbrication of the ore-hosting stratigraphy. This is also corroborated by estimates of the displacement of ore lenses along the Catherine and Railway faults established by underground structural mapping (Tessier and O'Donnell, 2001). This study reported maximum displacements of 100 to 400 m along individual splays, estimates that are too small to explain the km-scale duplication of the mine horizon.

East of the Ross Lake fault, five additional E-trending, S- to SE-dipping D4 thrust faults were modelled,

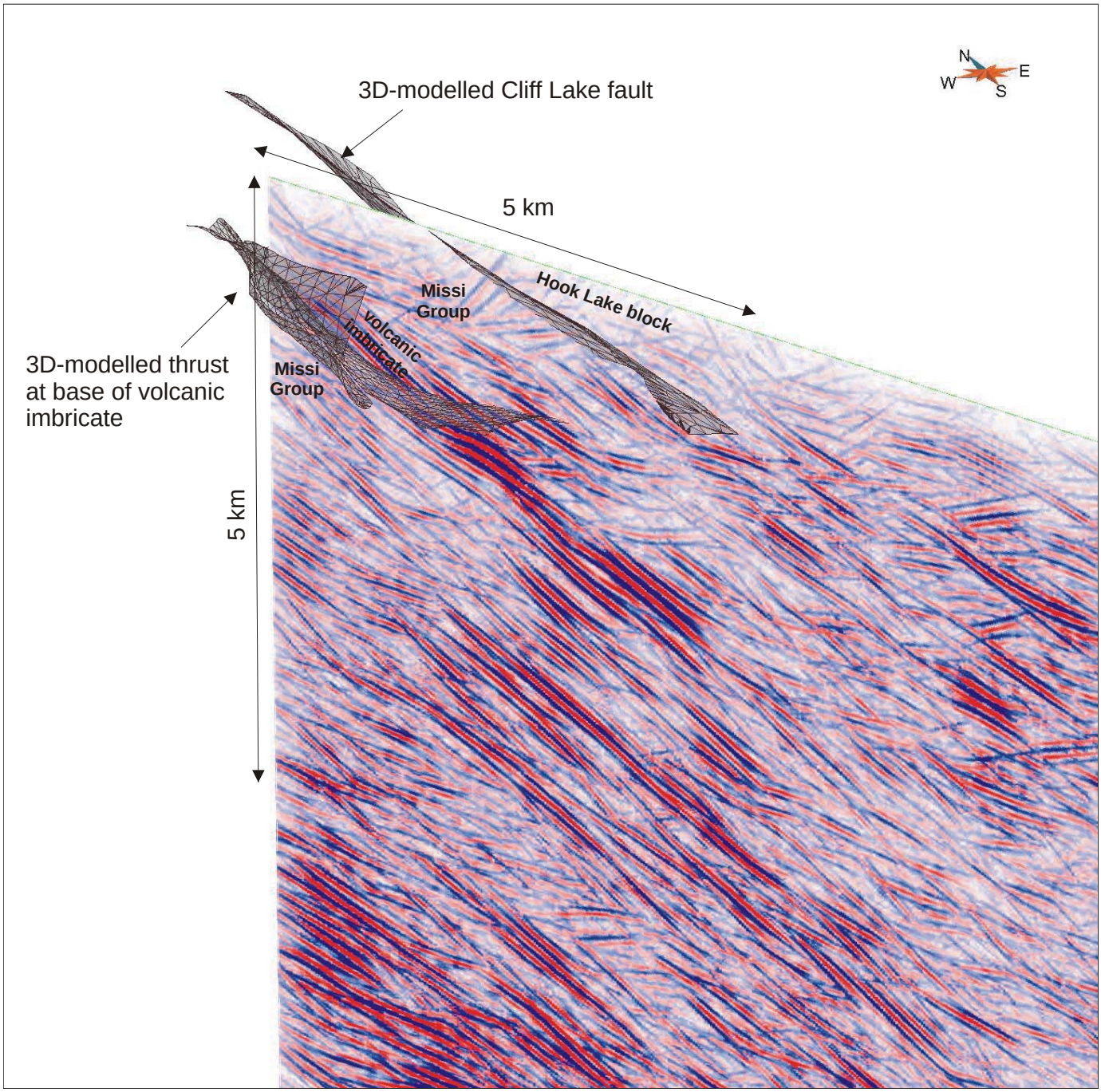

Figure 12. 3D perspective view of Lithoprobe migrated line 5 (Geological Survey of Canada) and 3D-modelled fault surfaces. Note that the geometry and dips of the 3D-modelled fault surfaces are concordant to bundles of moderately E-dipping regional seismic reflectors, suggesting that they define the bases of regionally E-dipping thrust-imbricates of Missi Group sedimentary- and Amisk collage volcanic arc rocks.

which imbricated Missi Group sedimentary rocks and the D3 thrust-imbricate of mafic volcanic and volcaniclastic rocks. The SE-dipping Lakeview thrust *[LakeViewThrust]* is constrained by its mapped surface trace and offsets in the imbricate of mafic volcanic rocks inferred from closely spaced drill holes.

Three blind thrust faults *[BlindMissiThrust1, BlindMissiThrust2, BlindMissiThrust3]* were inferred from the seismic interpretation of line 9 (Fig. 14; Malinoswki et al., *in prep.*) and the abrupt northward termination of the thrust-imbricate of volcanic rocks deduced from adjacent drill holes.

In exception to all the other S- to SSE-dipping thrust faults, there are no subsurface constraints to model the Birch View thrust fault *[BirchViewFault]*. As a result, only a tentative 3D model of this fault has been created by projecting its curvilinear surface trace to the subsurface, such that it truncates the Mud Lake syncline *[MudLakeSyncline]* and merges with one of the blind thrust faults *[BlindMissiThrust1]*.

Fold structures in the MissiGroup [FOLDF3F4MissiConglomerate]

Four folds structures developed in sedimentary rocks of the Missi Group were modelled, including the Flin Flon Creek, Pipe Line, Grant Lake and Mud Lake synclines. The synclines east of the Ross Lake fault, are all W-vergent structures with moderately E-dipping western and steeply E-dipping overturned eastern limbs. The geometry and asymmetry of these fold structures, which are particularly evident when viewed from the North (3DModel), appear to be consistent with W-vergent thrust faults imbricating the Flin Flon arc assemblage and the Missi structural basin. The model of the Pipe Line syncline shows complex interference of E-plunging F4 and SE-plunging F3 fold structures. It has a sheath fold geometry, suggesting that it was flattened and extended during the formation of the regional L5 stretching lineation (Lafrance et al., *in prep.*).

Post-metamorphic D7 subvertical faults [PostMetamorphicFaultsD7]

The Ross Lake and Channing faults *[RossLakeFault, ChanningFault]* (and reactivated Cliff Lake fault) are post-metamorphic NNW-trending subvertical brittle to ductile fault zones that segment the Missi structural basin, the Flin Flon block and the block of unassigned volcanic rocks and bound the Hook Lake block. Seismic reflectors from the seismic 2D lines and the 3D cube, corresponding to the unconformity between the Missi Group and Flin Flon arc-early successor arc basement and the thrust-imbricate of volcanic rocks, show significant fault offsets suggesting a sinistral-reverse sense of displacement consistent with previous kinematic inferences established by surface mapping (Fig. 6) (Gale et al., 1998 and references therein).

DISCUSSION AND CONCLUSIONS

An important consideration for VMS-targeting in the Flin Flon exploration camp hinges on the prediction of the regional subsurface extent and structural setting of the mine horizon (Millrock member). A preliminary hypothetical cross-section considered the Flin Flon-Callinan-777 VMS ore system and the Schist Mandy VMS deposits to be hosted in the upper mine horizon on opposite limbs of the Hidden Lake syncline based on similarities of the VMS-hosting lithostratigraphic successions and facing directions (Fig. 3). Although this schematic model portrays the repetition of the mine horizon, the intact synformal structure is, considering our 3D modelling results, highly unrealistic. Seismic interpretation and 3D modelling indicate that the Millrock member thrust-repeats, as well as the underlying units, retain their easterly dips to a depth of 2 km where they are truncated by the Ross Lake fault. The moderately 50^{o} - 60^{o} E-dipping 3D-modelled Millrock surfaces are aligned with regional E-dipping seismic reflectors that extend below the 2 km depth range (Fig. 10). This E-dipping depth projection of the mine horizon, however, does not preclude the presence of its lithostratigraphic equivalent above the 2 km depth range further east. On the contrary, the recognition of N-trending and E-dipping post-Missi thrust faults established by outcrop investigations (Lafrance et al., *in prep.*) and 3D modelling suggests that imbricated successions of the Flin Flon arc assemblage, including stratigraphic

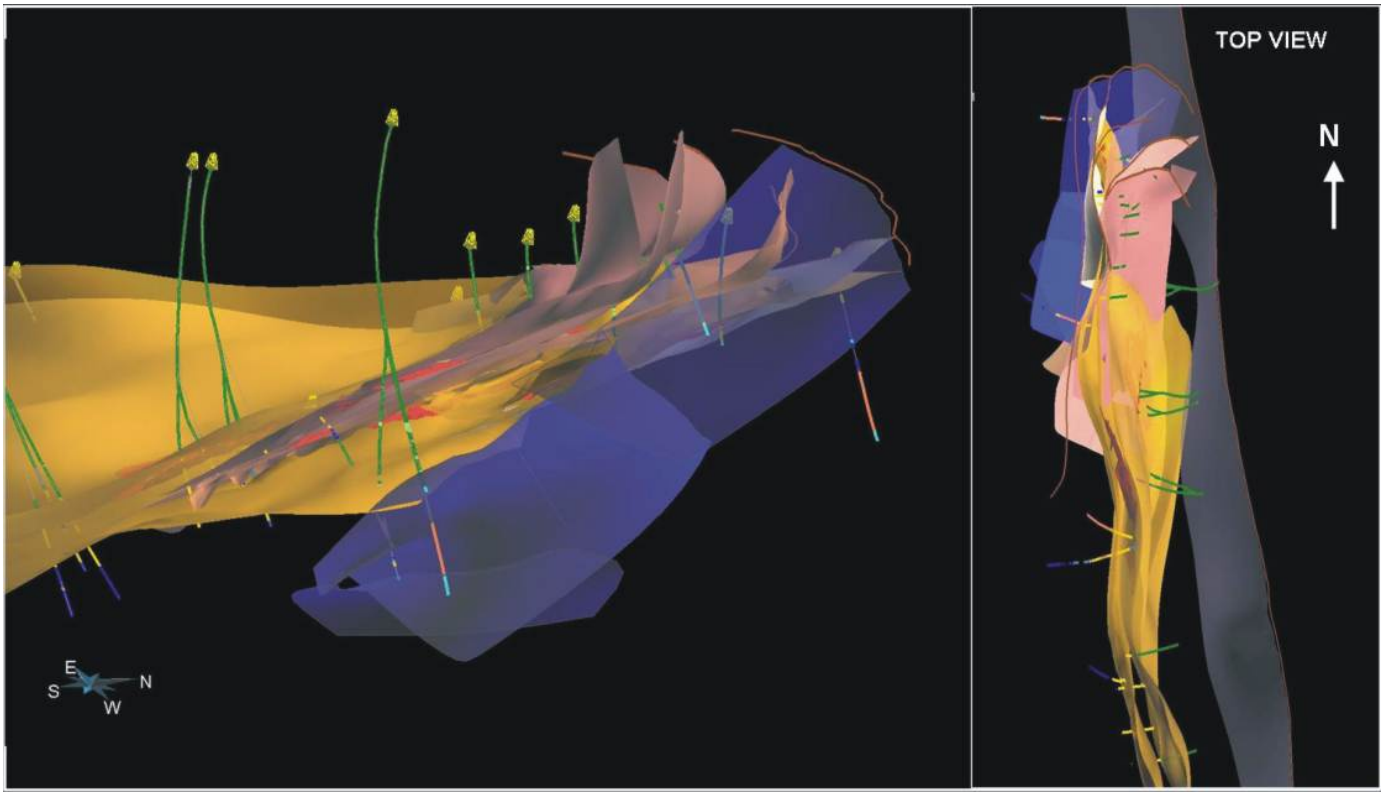

Figure 13. 3D model showing imbrication of the VMS-hosting Millrock member by Railway, Catherine and Club Lake thrust faults. Note how the Railway and Catherine faults (peach) imbricate the ore lenses (red) and how the faults surfaces intersect the earlier thrust-replicated Millrock member (yellow).

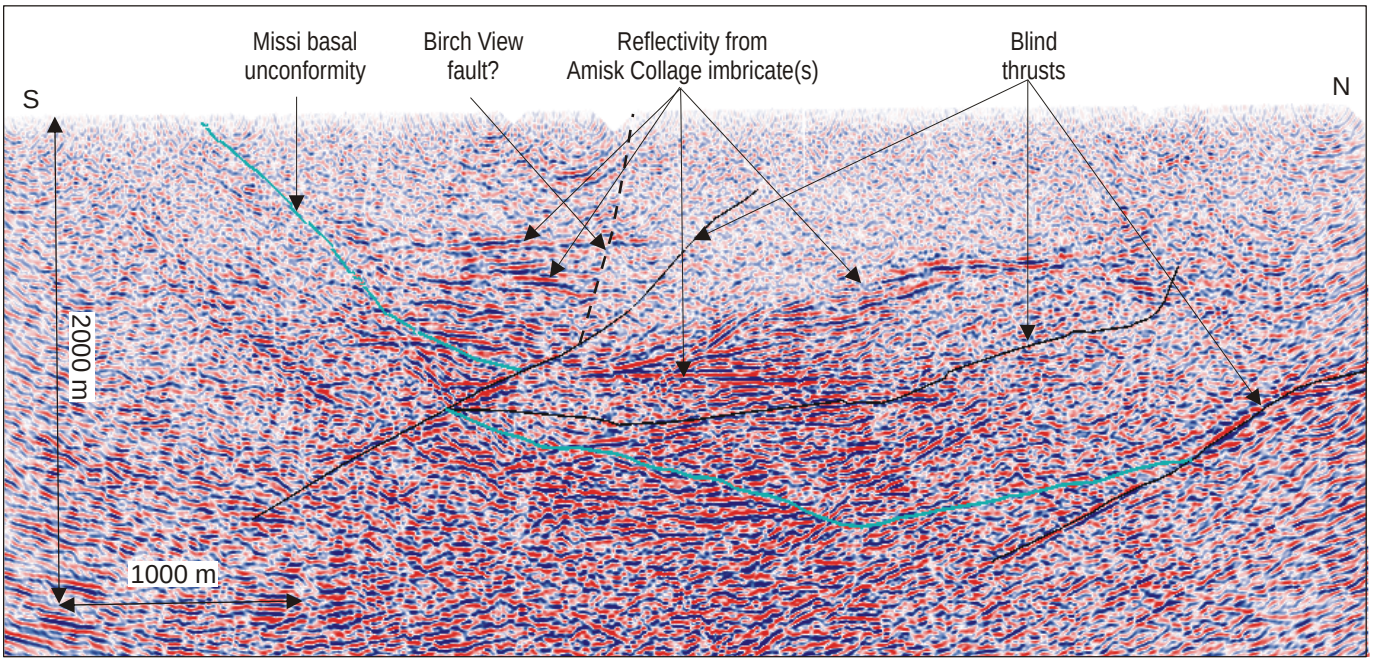

Figure 14. Migrated 2D seismic survey line 9 with superimposed seismic picks constraining 3D N-vergent, S-dipping blind thrusts that imbricate Missi sedimentary and Flin Flon arc assemblage mafic volcanic rocks.

equivalents of the mine horizon, can potentially be correlated across the Ross Lake, Channing and Cliff Lake faults. The generalized 3D picture is one of regionally E-dipping lithostratigraphic units involved in a thrust-imbricate architecture with only local preservation of fold hinges (Fig. 9) as opposed to an architecture defined by regionally continuous fold structures (Fig. 3). It should be emphasized that although our 3D geological model does not show regional D1 and D2 fold structures in the Flin Flon arc assemblage, we do not deny their existence. Regional F2 and F3 folds, however, were broken by multiple generations of N-trending faults and were preferentially developed internally within the lithostratigraphic formations of the Flin Flon arc assemblage (as opposed to involving their contacts). As a result the 3D geological model, being constrained by these lithostratigraphic contacts, is biased towards rendering the predominant homoclinal E-facing domains of the regional structure (Fig. 9).

The imbricate-thrust model expands the potential for the mine horizon to occur at multiple higher and/or lower structural levels throughout the Flin Flon exploration camp. The thrusting of Flin Flon arc assemblage rocks amidst sedimentary rocks of the Missi Group implies that the underexplored volume of Flin Flon arc basement underneath the Missi structural basin east of the Ross Lake fault, potentially hosts the eastern stratigraphic equivalent of the mine horizon at a similar or shallower depth range relative to the 777 deposit (Fig. 9; Fig. 10). The thrust-imbrication of mineralized hydrothermally-altered basalt (which perhaps is such an upthrusted stratigraphic equivalent or its immediate footwall), provides a second follow-up for exploration, since the mineralization, hosted within it, possibly extends from the 3D-modelled surface down-dip in the footwall of the Cliff Lake fault (Fig. 9). Another important implication for the structural understanding of the Flin Flon exploration camp unveiled by our 3D modelling efforts is that the thrust-imbricated architecture displays regional polyphase imbrication of the unconformity between the Missi Group and Flin Flon volcanic arc basement (Fig. 9; Fig. 12) contradicting the view of a largely intact fold-interference basin (Fig. 3).

The regional manifestation of post-Missi E-dipping thrust faults in our 3D-modelling results may also have important implications for the tectonic understanding of the western Flin Flon greenstone belt that has been regionally subdivided into NNW- to NNE-trending structural blocks with little to non-existent inter-block stratigraphic correlation due to early accretionary and/or post-collisional faulting (Lucas et al., 1999). Although to date this model provides a useful and robust tectonic framework for the Flin Flon greenstone belt (Syme, 2009), the geometry and kinematics of the tectonic relationships between individual blocks need to be critically examined. This holds particularly for block-bounding regional shear zones and faults that can not be conclusively assigned to early accretionary or exclusively post-collisional deformation events and that may, alternatively, have juxtaposed blocks by post-Missi thrusting during collisional stages of the Trans-Hudson orogeny. More regional 3D modelling work by intelligent integration of geological, seismic, potential field and drill hole data will be required to address this fundamental question.

A more local structural exploration guideline, deduced from the thrust-imbricated architecture of the 3D model, applies to the deposit scale in the vicinity of the Flin Flon Main, 777 and Callinan VMS ore system itself. The imbrication of E-dipping thrusts by N-vergent S- to SSE-dipping ductile shear zones has resulted in a complex tectonic stacking of the mine horizon with localized development of ductile shear fabrics in zones of intense hydrothermal alteration. This polyphase imbrication also undoubtedly contributed to the stacking of VMS ore lenses with the potential for undiscovered VMS lenses to occur in the near vicinity of the known deposits at both deeper and shallower structural levels. A newly discovered 0.25 Mt high-grade zone of mineralization in the footwall of the 777 deposit (*pers. comm.* HudBay Minerals Inc.), adding a fourth level of thrust-imbrication, supports this interpretation.

ACKNOWLEDGEMENTS

The 3D model of the Flin Flon exploration camp is the product of a joint and multi-disciplinary effort of geologists, geophysicists, geochemists and GIS experts participating in the TGI3 Flin Flon project. Kelly Gilmore, Jason Levers and Brett Pearson are thanked for their hospitality, logistical support and sharing their expertise in the underground geology of the Flin Flon-Callinan-777 VMS ore system. We would also like to thank David Price for guiding us to outcrops that were essential in gaining a 3D understanding in the geology of the Flin Flon mine camp. Bruno Lafrance is gratefully acknowledged for sharing his insight on the structural geology of the Flin Flon exploration camp and providing his high-quality structural measurements that made it possible to model the fold structures in the Missi structural basin in three dimensions. Richard Allmendinger's StereoWin v. 1.2 program was used for stereographic plotting and statistical analysis of bedding elements. Renée-Luce Simard, Kate MacLachlan, Doreen Ames and Harold Gibson are thanked for sharing their knowledge obtained through detailed surface mapping and insightful discussions. Alan Galley and Eric de Kemp are acknowledged for thoughtful reviews of this manuscript. Kathryn Coyle is thanked for proofreading the text and testing the 3D interactive model included in this report. This is GSC contribution OF6313.

REFERENCES

Ames, D. E., Tardif, N., MacLachlan, K. and Gibson, H. L. 2002. Geology and hydrothermal alteration of the hanging wall stratigraphy to the Flin Flon-777-Callinan volcanogenic massive sulphide horizon (NTS 63K12NW and 13SW), Flin Flon area, Manitoba; in Report of Activities 2002, Manitoba Industry, Trade and Mines - Geological Services, pp. 20-34.

Ames, D. E., Tardif, N., Galley, A. G., Gibson, H. L. and MacLachlan, K. 2003. Hanging wall stratigraphy and hydrothermal signature of the Paleoproterozoic Flin Flon-Triple 7-Callinan VMS deposits; FF-TGI; Geological Association of Canada; Mineralogical Association of Canada, Vancouver, Program with abstracts, v. 28,

Bailes, A.H. and Syme, E.C. 1989. Geology of the Flin Flon – White Lake area; Manitoba Energy Mines, Geol. Rep. GR87-1. 313 p.

Cole, E.M., Piercey, S.J. and Gibson, H.L. 2008. Geology and geochemistry of the Schist Lake mine area, Flin Flon, Manitoba (part of NTS 63K12); *in* Report of Activities 2008, Manitoba Science, Technology, Energy and Mines, Manitoba Geological Survey, pp. 18-28.

Corrigan, D., Pehrsson, S., Wodicka, N. and de Kemp, E. 2009. The Paleoproterozoic Trans-Hudson Orogen: a prototype of modern accretionary processes. Journal of the Geological Society of London, Special Volume "Ancient Orogens and Modern Analogues". From: MURPHY, J. B., KEPPIE, J. D. & HYNES, A. J. (eds.) Ancient Orogens and Modern Analogues. Geological Society, London, Special Publications, v. 327, pp. 457-479.

Devine, C.A., Gibson, H.L., Bailes, A.H., MacLachlan, K., Gilmore, K. and Galley, A.G. 2002. Stratigraphy of VMS-hosting volcanic and volcaniclastic rocks of the Flin Flon Formation, Flin Flin-Creighton area, Saskatchewan and Manitoba *in* Summary of Investigations 2002 v. 2, Saskatchewan Geological Survey, Sask. Industry Resources, Misc. Rep. 2002-4.2, CD-ROM, Paper B-4, 11p.

Devine, C. 2003. Origin and emplacement of volcanogenic massive sulphide-hosting, Paleoproterozoic volcaniclastic and effusive rocks within the Flin Flon subsidence structure, Manitoba and Saskatchewan, Canada; M.Sc. thesis, Laurentian University, Sudbury, 279 p.

DeWolfe, Y. M. 2008. Physical volcanology, petrology and tectonic setting of intermediate and mafic volcanic and intrusive rocks in the Flin Flon volcanogenic massive sulphide (VMS) district, Manitoba, Canada: Growth of a Paleoproterozoic juvenile arc; Ph.D. thesis, Laurentian University, Sudbury, 269 p.

Farin, G. 1988. Curves and surfaces for computer-aided geometric design, a practical guide, Academic Press, san Diego, 334 p.

Gale, D. F., Lucas, S.B. and Dixon, J.M. 1998. Structural relations between the polydeformed Flin Flon arc assemblage and Missi Group sedimentary rock, Flin Flon area, Manitoba and Saskatchewan. Canadian Journal of Earth Sciences v. 36, pp. 1901-1915.

Galley, A. G., Syme, E.C. and Bailes, A.H. 2007. Metallogeny of the Paleoproterozoic Flin Flon Belt, Manitoba and Sakatchewan *in* Goodfellow, W.D. ed., Mineral deposits of Canada: A synthesis of major deposit types, district metallogeny, the evolution of geological provinces and exploration methods: Geological Association of Canada, Mineral Deposit Division, Special Publication No. 5, pp. 509-531.

Geological Survey of Canada, Lithoprobe Data archive, Seismic data Trans Hudson (THOT) http://edg.rncan.gc.ca/seismtlitho/archive/thot/index_e.php.

Gibson, H. L., Devine, C., Galley, A. G., Bailes, A. H., Gilmore, K., MacLachlan, K. and Ames, D. E. 2003. Structural control on the location and formation of Paleoproterozoic massive sulfide deposits as indicated by synvolcanic dyke swarms and peperite, Flin Flon, Manitoba and Saskatchewan; Geological Association of Canada; Mineralogical Association of Canada, Vancouver, Program with abstracts, v. 28.

Gibson, H.L., Lafrance, B., DeWolfe, M., Devine, C., Gilmore, K., Pehrsson, S. 2009. Volcanic reconstruction and post depositional modification of a cauldron subsidence structure within the Flin Flon VMS District. Prospectors and Development Association of Canada (PDAC) technical session presentation: Flin Flon: new developments in an old camp, Toronto, 2 March 2009. http://www.pdac.ca/pdac/conv/2009/pdf/tech-session/ts-gibson.pdf

Kremer, P.D. and Simard, R-L. 2007. Geology of the Hook Lake Block, Flin Flon area, Manitoba (part of NTS 63K12); *in* Report of Activities 2007, Manitoba Science, Technology, Energy and Mines, Manitoba Geological Survey, pp. 21-32.

Lafrance, B., Gibson, H.L. DeWolfe, M., Pehrsson, S., Schetselaar, E., Rayner, N. And Lewis, D. 2010. Structural reconstruction of the Flin Flon volcanogenic massive sulfide mining district, Saskatchewan and Manitoba, Canada (*in prep.*).

Lewis, D., Lafrance, B., MacLachlan, K. and Gibson, H. 2006. Structural investigations of Millrock Hill and the hinge zone of the Beaver Road Anticline, Creighton, Saskatchewan: in summary of Investigations 2006. Saskatchewan Geological Survey, Sask, Industry Resources, Mics. Rep. 2006-4.2, CD-ROM, Paper A-10. v. 2. 11p.

Lucas, S.B., Syme, E.C., Reilly, B.A., 1995. Structural history of long-lived shear zones in the central Flin Flon Belt, eastern Trans-Hudson Orogen *in* Hajnal, Z. and Lewry, J. (*eds.*) Lithoprobe Trans-Hudson Orogen Transect, Report No. 48. pp. 170-186.

Lucas, S.B., Stern, R.A., Reilly, B.A., Thomas, D.J. 1996. Intraoceanic tectonics and the development of continental crust; 1.92- 1.84 Ga evolution of the Flin Flon belt, Canada, Bulletin of the Geological association of America, v. 108, no. 5, pp. 602-629.

Lucas, S.B., Syme, E.C. and Ashton, K.E., 1999. New perspectives on the Flin Flon Belt, Trans-Hudson Orogen, Manitoba and Saskatchewan: an introduction to the special issue on the NATMAP Shield Margin Project, Part 1., Canadian Journal of Earth Sciences, v. 36, pp. 135-140.

Malinowski, M, White, D.J. Pehrsson, S., Schetselaar, E, Salisbury, M. and Mwenifumbo J. 2010. Seismic imaging of the Flin Flon VMS mining camp, Trans-Hudson Orogen, Canada (*in prep.*).

Mallet, J.L. 1992. Discrete smooth interpolation in geometric modelling. Computer-Aided Design, 24 no. 4, pp. 177-191.

MacLachlan, K. and Devine, C., 2007. Stratigraphic Evidence for Volcanic Architecture in the Flin Flon Mining Camp: Implications for Mineral Exploration in Summary of Investigations 2007 v. 2, Saskatchewan Geological Survey, Sask. Industry Resources, Misc. Rep. 2007-4.2, CD-ROM, Paper A-1, 29 p.

Renard R. and Courrioux, G. 1994. Three-dimensional geometric modeling of a faulted domain: The Soultz Horst example (Alsace, France) Computers & Geosciences, v.20, pp. 1379-1390.

Rayner, N., 2010. New U-Pb zircon ages from the Flin Flon Targeted Geoscience Initiative Project 2006-2009: Flin Flon and Hook Lake blocks, Manitoba and Saskatchewan; Geological Survey of Canada, Current Research 2010-4, 12 p.

Ryan, J. and Williams, P., 1999. Structural evolution of the eastern Amisk collage, Trans-Hudson Orogen, Manitoba, Canadian Journal of Earth Sciences, v.36, pp. 251-273.

Schetselaar, E., deKemp, A. and Hillier, M. 2010. Method development for green-fields to deposit-scale 3D modelling illustrated with case studies from TGI3 project areas, Geological Association of Canada TGI3 workshop: public geoscience in support of base metal exploration abstract, Vancouver 22 March 2010. http://www.gac-cs.ca/workshops/TGI3/abstracts/02_GAC_TGI3_Schetselaar_3D_modeling.pdf

Simard, R-L. 2006. Geology of the Schist Lake-Mandy mines area, Flin Flon, Manitoba (part of NTS 63K12); *in* Report of Activities 2006, Manitoba Science Technology, Energy and Mines, Manitoba Geological Survey, pp. 9-21.

Simard, R-L., MacLachlan, K., Gibson, H.L., DeWolfe, Y.M., Devine, C., Kremer, P.D., Lafrance, B., Ames, D.E., Syme, E.C., Bailes, A.H., Bailey, K., Price, D., Pehrsson, S., Cole, E., Lewis, D. and Galley, A.G. 2010. Geology of the Flin Flon area, Manitoba and Saskatchewan (part of NTS 63K12, 13); Manitoba Innovation, Energy and Mines, Manitoba Geological Survey, Geoscientific Map MAP2010-1 and Saskatchewan Ministry of Energy and Resources, Geoscience Map 2010-2, 1 colour map, scale 1:10000.

Sprague, K. B. and de Kemp E. A. 2005. Interpretive tools for 3-D structural geological modelling part II: surface design from sparse spatial data. Geoinformatica v. 9 no. 1, pp. 5-32.

Stauffer, M.R. and Mukherjee, A. 1971. Superimposed deformations in the Missi metasedimentary rocks near FlinFlon, Manitoba. Canadian Journal of Earth Sciences, v. 8, pp. 217-242.

Stern, R.A., Syme, E.C. and Lucas, S.B. 1995. Geochemistry of 1.9 Ga MORB- and OIB-like basalts from the Amisk collage, Flin Flon belt, Canada: evidence for an intra-oceanic origin. Geochimica et Cosmochimica acta, 59, pp. 3131-3154.

Stern, R.A., Machado, N., Syme, E.C., Lucas, S.B., David, J. 1999. Chronology of crustal growth and recycling in the Paleoproterozoic Amisk collage (Flin Flon Belt), Trans-Hudson Orogen, Canada. Canadian Journal of Earth Sciences, v. 36, pp. 1807-1827.

Stockwell, C.H. 1960. Flin Flon-Mandy area, Manitoba and Saskatchewan. Geological survey of Canada, Map 1087 A.

Syme, E.C. and Bailes A.H. 1993. Stratigraphic and tectonic setting of Early Proterozoic volcanogenic massive sulphide deposits, Flin Flon, Manitoba. Economic Geology v. 88, no. 3, pp. 566-589.

Syme, E.C., Lucas, S.B., Bailes, A.H., Stern, R.A. 1999. Contrasting arc and MORB-like assemblages in the Paleoproterozoic Flin Flon Belt, Manitoba, and the role of intra-arc extension in localizing volcanic-hosted massive sulphide deposits. Canadian Journal of Earth Sciences v. 36, pp. 1767-1788.

Syme, E.C. 2009. The Flin Flon greenstone belt: history of an outstanding Paleoproterozoic collage and VMS district. Prospectors and Development Association of Canada (PDAC) technical session presentation: Flin Flon: new developments in an old camp, Toronto, 2 March 2009. http://www.pdac.ca/pdac/conv/2009/pdf/tech-session/ts-syme.pdf

Tessier, A.C. and O'Donnell (2001) Callinan/777 Deposit. Compilation and Target Generation Project, unpublished report, Hudson Bay Mining and Smelting Co. 154 p.

Appendix 1: Instructions to interact with the Flin Flon 3D Knowledge Cube in Acrobat™ 3D .PDF format.

This Open File report contains the Flin Flon 3D knowledge cube in Acrobat™ .PDF format (3DModel) that allows readers interacting with its 3D elements using the model description on p. 21 as a guide. This appendix provides some basic instructions for viewing and interacting with the 3D model. Reference is made to the Acrobat™ help functions for more details.

Supported format
The 3D model can be opened using Acrobat™ Reader 7.0 and higher versions.

Preferred settings
Make sure that the 'enable double-sided rendering' option is selected (found under 'Edit', 'Preferences')

Accessing the 3D model
The 3D model does not have to be opened by the user. Simply scroll to the page that contains the 3D model and click on the 3D model to interact with it. Note that it takes some time to load the 3D model in memory (typically 30 s to 1 minute on most computers).

Navigation
Use the hand tool for navigation (if the icon is not displayed it can be found under 'Tools', 'Select & Zoom').
The following navigation functions are available:

left mouse button: rotate
right mouse button: zoom in/zoom out
left/right mouse buttons together: pan

View table of contents and object selection

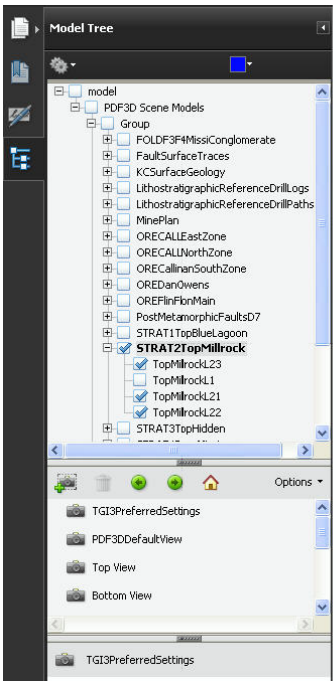

Open the model tree for an overview of the model elements in the file. If the model tree icon is not displayed, select: 'View', 'Navigation Panels', 'Model Tree' from the top menu.

A hierarchically-organized table of contents is displayed in the Model Tree. Check/ uncheck the boxes in front of the listed model elements to display/hide the model elements. Click the + button of the Model Tree to browse to deeper levels in the object hierarchy.

By clicking and holding the right-mouse button on individual objects or groups of objects in the model tree, the display settings of model elements can be modified using the 'part render mode' option. Suitable options for displaying the elements of the 3D knowledge cube are: 'solid', 'transparent' and 'wireframe'.

Selecting views
Different 'Views' indicated with camera icons are displayed underneath the Model Tree. These views define the directions from which the 3D model is rendered (top, bottom, north, south, east, and west), which model elements are rendered and how model elements are rendered (transparent, etc.).

The 3D view can be centered one or more objects of interest by selecting one of them in the model tree, holding the right mouse button and selecting the option "fit visible"

Changing the background colour and lighting schemes
The background colour and lighting schemes (and various other settings) can be adapted by clicking with the right-mouse button on the 3D model window and selecting the 'viewing options'. The drill hole elements are optimally rendered against a black background.